The Effects of Sleep Deprivation on Brain's Functional Integration and Segregation

Mohadeseh Panahi Moghadam

A Thesis

in

The Department

of

Electrical and Computer Engineering

Presented in Partial Fulfillment of the Requirements

for the Degree of

Master of Applied Science (Electrical and Computer Engineering) at

Concordia University

Montréal, Québec, Canada

December 2022

CONCORDIA UNIVERSITY

School of Graduate Studies

This is to certify that the thesis prepared

By: **Mohadeseh Panahi Moghadam**

Entitled: **The Effects of Sleep Deprivation on Brain's Functional Integration and Segregation**

and submitted in partial fulfillment of the requirements for the degree of

Master of Applied Science (Electrical and Computer Engineering)

complies with the regulations of this University and meets the accepted standards with respect to originality and quality.

Signed by the Final Examining Committee:

_____ Chair
Dr. Arash Mohammadi

_____ External Examiner
Dr. Christophe Grova

_____ Examiner
Dr. Hassan Rivaz

_____ Supervisor
Dr. Habib Benali

Approved by _____
Dr. Yousef R. Shayan, Chair
Department of Electrical and Computer Engineering

_____ 2022   _____
Dr. Mourad Debbabi, Dean
Faculty of Engineering and Computer Science

Abstract

The Effects of Sleep Deprivation on Brain's Functional Integration and Segregation

Mohadeseh Panahi Moghadam

Brain is a complex system that contains multiple localized groups each of which performs independent tasks. Nevertheless, the brain can also run as a unique system that its function depends on different localized groups. These two principles of the brain are called functional segregation and integration, respectively, and there should be a balance between them for the brain to act properly. In this thesis, we hypothesized that sleep deprivation might have a negative effect on these principles which results in loss of sustained attention and having difficulty performing tasks. Moreover, we investigated the effects of the circadian rhythm and homeostatic sleep pressure on functional integration. Another hypothesis was that if a part of the fMRI time-series is not stationary, the results of the functional integration might not be reliable. Total integration, between-network integration and within-network integration were measured using the fMRI data set provided by our colleagues from University of Liège. Our results show that global integration increased after sleep deprivation while the segregation decreased, and integration's maximum level was around the peak of the melatonin curve for each subject. Furthermore, in a non-stationary fMRI signal, numerous fluctuations were found in the integration results compared to when the signal was stationary.

Acknowledgments

The journey of life has been always full of wonders and unexpected events. I am happy that in this journey, I had the opportunity to work under Dr. Habib Benali's supervision who has been a great supporter, a family-like teacher, and a caring human being. I learned a lot from him and my peers while I was in Dr. Benali's research team, the Biomedical Imaging for Healthy Aging Laboratory. So, I would like to express my deepest appreciation to Dr. Benali.

I would also like to express my gratitude to Amanda Robinson who trusted me and offered me her support when I needed help. Moreover, I am very grateful to my best friend Francesco Francissen who has always encouraged and supported me and given me fatherly advice.

I could not have undertaken this journey without the emotional support that I received from my beloved family, my sisters who are the joy of my life, my mother who always gives me hope and it is for her that I resist during hardships, and my father for whom I was inspired to become an engineer and he will always remain in my heart. You are all the most beautiful treasures that I have in this life.

I would like to extend my sincere thanks to the people of my country, Iran. You inspired me more than anyone else. Since the death of Mahsa Amini in September 2022, I cried and laughed with you, checked your news every second, prayed for you, and my eyes and attention were just fixated on you. I saw how courageous you are when you stood up barehanded in front of gunshots and oppression. From your bravery, I learned to become a better person, I learned how to care about others, and I deeply understand that when you are in pain, I am in pain too. So, we continue together until we are all free and happy.

Finally, I want to dedicate a few lines to a 10 years old boy called Kian Pirfalak who said "In the

name of the rainbow's God" when he was introducing his handmade wooden boat. He wanted to become a robotics engineer. But sadly, his life was taken before he could achieve this dream. Dear Kian, I am sure that because of your innocence and pure soul, the world will become a better place and the God of the rainbow will save all people who are experiencing such cruelties and bestows colorful lives upon everyone. We will never forget you.

In the name of the rainbow's God *** The merciful and kind God

Shall Khodanoor who was the light of God *** Get awakened in people's hearts!

For Women, Life, Freedom!

For Men, Children, Humanity!

Contents

List of Figures

List of Tables

Abbreviations

ADF Augmented Dickey-Fuller.

ANOVA Analysis of Variance.

AR Auto-Regressive.

AR(1) First-order AR.

AR(2) Second-order AR.

ARD Autoregressive model with Drift variant.

BOLD Blood Oxygenation Level Dependent.

CCTV Closed-Circuit Television.

CR Constant Routine.

DF Dickey-Fuller.

EEG Electroencephalography.

EPI Echo-Planar Imaging.

ESS Epworth Sleepiness Scale.

FCR Functional Clustering Ratio.

fMRI Functional Magnetic Resonance Imaging.

FWHM Full Width at Half Maximum.

GLM Generalized Linear Model.

Hb Hemoglobin.

HI Hierarchical Integration.

HRF Hemodynamic Response Function.

KL Kullback–Leibler.

KSS Karolinska Sleepiness Scale.

LGG Low-Grade Glioma.

LS Least-Square.

MIST Multiresolution Intrinsic Segmentation Template.

MNI Montreal Neurological Institute.

MRI Magnetic Resonance Imaging.

MSTEPS Multiscale Stepwise Selection Algorithm.

NaN Not a Number.

NREM Non-Rapid Eye Movement.

PP Phillips-Perron.

PSG Polysomnography.

PSQI Pittsburgh Sleep Quality Index.

PVT Psychomotor Vigilance Task.

RF Radio Frequency.

ROI Region-of-Interest.

rs-fMRI Resting-State fMRI.

SCN Suprachiasmatic Nucleus.

SD Sleep Deprivation.

SHY Synaptic Homeostasis Hypothesis.

SNR Signal-to-Noise Ratio.

SPM Statistical Parametric Mapping.

SWA Slow Wave Activity.

t-fMRI Task-Based fMRI.

TS Trend-Stationary model variant.

WSS Weak-Sense Stationary.

Chapter 1

Introduction

Chapter 1 provides complete definitions on functional segregation and integration, sleep regulation and sleep deprivation. Moreover, in this chapter, the goal of this research is explained.

1.1 Functional Segregation and Integration

The brain consists of several areas which perform specific tasks. Higher species have extremely complex brains in which there is always an immense flow of information between different neuronal groups that have specialized functions. The information from these groups which are located in distinct regions of the brain are integrated and together, they have a meaningful function [1]. The link between two neurons in different groups creates a reciprocal route to which neurons can enter multiple times and as a result, global correlation patterns between these groups appear [2]. This global function of the neuronal groups which is called functional integration occurs at all the times; during wakefulness, during sleep, while dreaming, etc. [1].

As the functions of distinct brain regions are dissimilar, we can say there is functional segregation and modularity in the brain. This means that different tasks are assigned to specific brain regions. For example, to understand shape and color of an object, there exists different brain regions which perform each of these tasks separately [1].

The functional brain balances these two principles, functional integration and functional segregation which are shown in Figure 1.1, harmoniously to be as efficient as possible. If the activities of

some neuronal groups are independent from each other, we can say they are functionally segregated. On the other hand, if their activities are statistically dependent on each other, they are functionally integrated [2].

Functional segregation   Functional integration
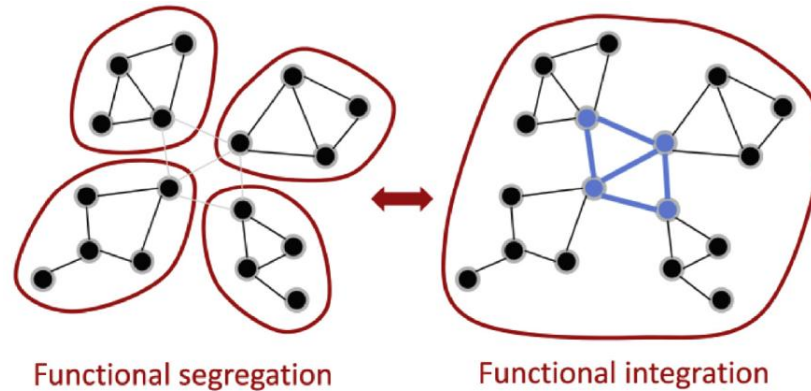
Figure 1.1: Functional Segregation VS. Functional Integration [3]
.

1.2 Sleep Regulation

Having enough sleep during each day is as vital to survival as food and water. But why do we need to sleep and disconnect from the world for one third of each day in our lives? In [4], Tononi and colleagues proposed that according to the Synaptic Homeostasis Hypothesis (SHY), plasticity is the main reason for which our brain needs sleep. During wakefulness, we obtain more information about our surroundings [5]. For all that new information, new connections would be created inside the brain. This process takes energy and at some point, the Signal-to-Noise Ratio (SNR) decreases, and it becomes hard to learn more. Sleep after a long day of learning helps in memory consolidation, renormalizing the strength of the synapses and restoring the energy required for learning [4].

Sleep deprivation can lead to minor or major disorders from irritability and tiredness to depression, diabetes, high blood pressure, etc. Although it is true that having a good sleep freshens the brain and helps it function well, it is worth understanding what is being restored to the brain during sleep. As mentioned, SHY explains that during wakefulness, as we learn new knowledge, our synapses would need more supplies, and while asleep, synapses form between neurons. As shown

in Figure 1.2, brain needs to consume additional energy to increase the synaptic strength and learning more expands the cellular stress and at some point, we are not able to learn more. At this level, brain needs sleep which reduces the cellular stress, restores the supplies and desaturates the plasticity which leads in restoration of the learning capability and improvement of the SNR. In summary, it will result in the memory consolidation and integration. This restoration of synaptic homeostasis is the main reason that the brain needs sleep as SHY proposes [4].
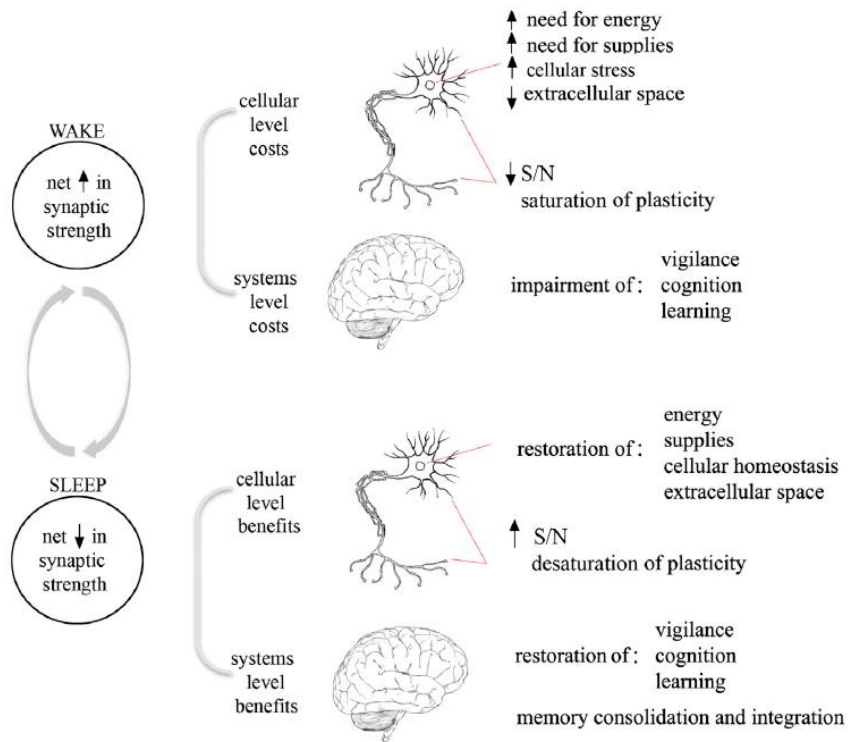
Figure 1.2: The Synaptic Homeostasis Hypothesis or SHY [4]
.

In the following sections, two factors that make us feel sleepy at certain times of the day are explained.

1.2.1   Circadian Rhythm

The first factor that makes us feel sleepy is related to the circadian rhythm. There is a small region in the brain called the hypothalamus which contains some nerve cells. These groups of cells

affect the functions of awakening and sleeping depending on the day-night cycle. The Suprachias-matic Nucleus (SCN) is inside the hypothalamus and acts as the master clock of the brain. Through our eyes, SCN is signalled about the light exposure and controls for this 24-h cycle which is called the circadian rhythm. Hypothalamus and the brain stem work together to control the pathway from wakefulness to sleep or vice versa. Also, a brain chemical called GABA will be produced by them to decrease the activities of arousal centers in the brain [6].
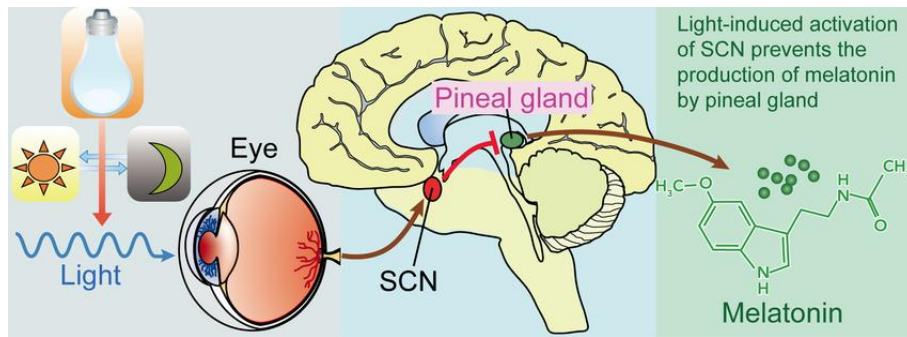
Figure 1.3: The effect of light in the production of melatonin [7]
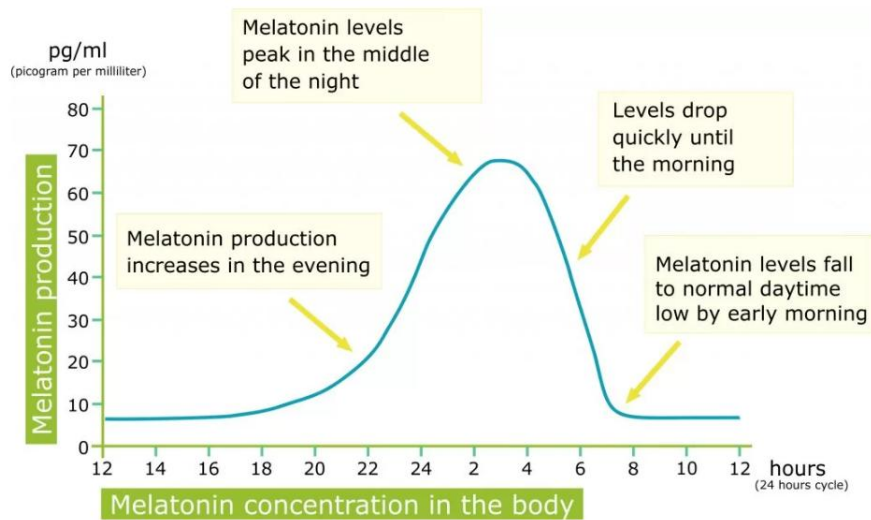
Figure 1.4: The cycle of melatonin's production in 24 hours [8]

Later in the evening, when the daylight is decreasing, the SCN sends signals to a region within the brain's two hemispheres called pineal gland to produce a hormone called melatonin. This hormone helps regulate the timing of sleep but does not actively participate in generating sleep (Figure 1.3). The concentration of melatonin increases in the evening and in the morning, its production

4

stops due to the morning light (Figure 1.4).

So, circadian rhythm is a reason that night shift workers or people who fly to a different time zone often have insomnia. Their body's clock would be different from the actual clock [6].

1.2.2 Sleep Pressure

The second factor that determines the time for sleep is related to the homeostasis. There is a chemical substance called adenosine which is released from cells in basal forebrain that is a region in the brain. An increase in adenosine increases the body's need for sleep which is called a homeostatic sleep pressure or sleep drive. This sleep pressure grows while the person is still sleep deprived, but when the person sleeps or has a short nap, the sleep pressure declines (Figure 1.5). Caffeine does not let adenosine act properly. It neutralizes the sleep pressure and makes us feel refreshed [6].
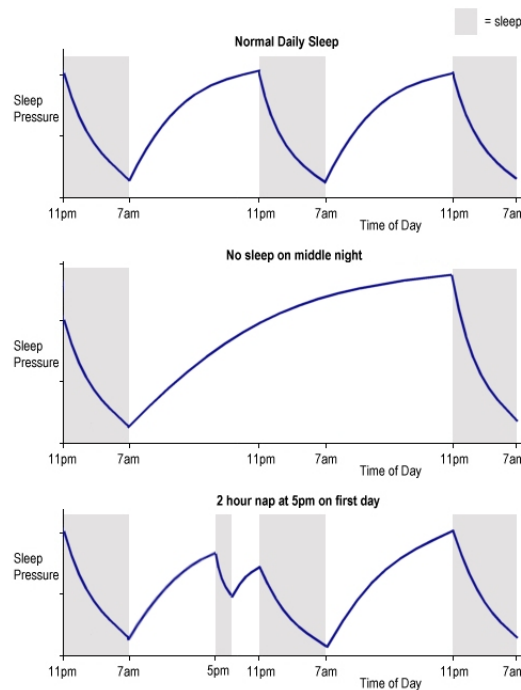
Figure 1.5: The sleep pressure during wakefulness and sleep [9]

1.2.3 The Two-Process Model

A model named the two-process model (Figure 1.6) was proposed in [10] for sleep regulation. In this model, it is proved that a homeostatic process (named as Process S) and another process which

5

is guided by the circadian pacemaker (named as Process C) have interactions during different time periods. As discussed, Process S which represents the sleep pressure increases while sleep deprived and once asleep, it decreases. When Process S is near a certain minimum threshold, it signals the brain for awakening and when it reaches a high threshold, it signals the brain for sleeping. The marker of Process S during sleep is the Electroencephalography (EEG) Slow Wave Activity (SWA) in Non-Rapid Eye Movement (NREM) sleep and during wakefulness, theta activity is its marker.

Process C represents the circadian rhythm and it has a clock-like mechanism. It does not depend on the prior sleeping and waking habits. As explained in section 1.2.1, it has its own rhythm which is affected by light, and at certain times of a day, people have higher or lower tendency to sleep [10]. The markers for the Process C are the melatonin and the body temperature levels [11].
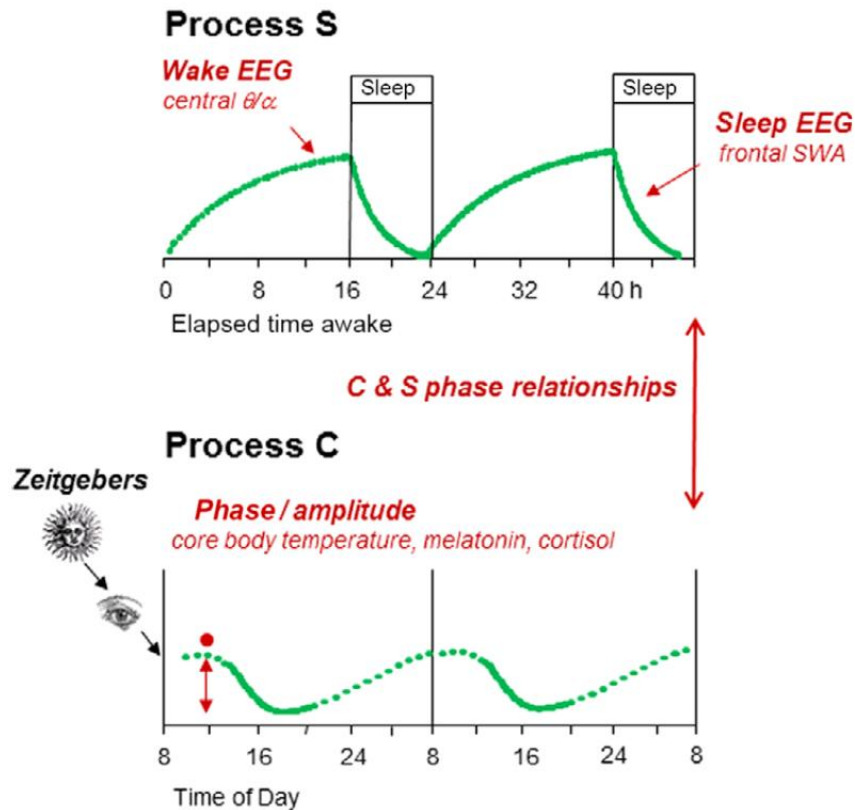
Figure 1.6: The schematic of the two-process model [11]

In animal experiments in [10], it is shown that when sleep deprived, Process S continues even after disrupting Process C by lesioning the SCN. In another study, it was proved that by changing the circadian phase of Process C, Process S remained unaltered which suggests that one of these

6

processes can be independently controlled [10] and they regulate separately [11].

1.3 Sleep Deprivation

Sleep Deprivation (SD) can drastically affect the quality of life [12] and may cause some disorders. Some people may think of sleep as an unnecessary part of their lives and wish they could use that time for studying, working, or doing a more meaningful task instead of sleeping. Apart from this, in some professions such as health care, military, or night-shift workers, not having adequate sleep is very normal and part of their jobs. Obtaining more knowledge about the importance of sleep and consequences of sleep deprivation on one hand can enlighten us about the benefits of this function and on the other hand, it will help us in improving the quality of our lives and caring more about our well-being by getting enough sleep each day [13].

There are two forms of sleep deprivation, total and partial SD. In total SD, the subjects are not allowed to sleep for more than 24 hours. While in partial SD, the subjects can have a short nap at some specified times during the experiment. The partial SD is more common in the real life, and it is worth being explored more thoroughly [12]. Both conditions can impose many negative effects on our lives and reduce our cognitive performances. A normal night's sleep can be between 7 and 8.5 hours per day, but depending on each individual's sleeping habits, the length of sleep can be more or less [12]. When studying the effects of SD, factors such as age, gender and dissimilarities between the individuals should be considered. Moreover, in SD experiments, the protocol should contain a recovery process from SD for the subjects [13]. The effects of SD also vary for each person. But in most subjects, total SD harms attention, working memory and decision-making, and partial SD can negatively affect the vigilance attention [12]. It is shown that most of these changes are related to the prefrontal areas and limbic system regions such as the amygdala and hippocampus [13]. SD also alters people's mood and emotions. It can make a person feel more stressed, irritable, and aggressive, and even make him have suicidal thoughts. Sleep is essential in forming new memories [14]. So, when sleep deprived, the hippocampus's duty in encoding episodic memory would be influenced. SD can also reduce the activity and change functional connectivity in the attention [15] and salience networks [16].

Some resting-state studies have shown the effects of SD on the connectivity profiles of the subjects in many brain regions and networks such as the default mode, dorsal attention, auditory, visual and motor networks [15, 17, 18]. In a 36-hour of SD experiment, it was shown that even without performing any tasks, there were changes in the connectivity of amygdala [19]. In another resting study, the change in vigilance is proved by demonstrating the reduction in thalamic connectivity [17]. In [17], the effects of SD were analysed in 18 subjects using rs-fMRI. They used graph theory method to study how functional segregation changes in sleep deprivation and they proved that apart from the reduction in some networks' functional connectivity, the modularity formation of the brain would also decrease. In a partial SD resting-state fMRI experiment [20], the connectivity between the dorsal nexus and the dorsolateral prefrontal cortex was increased. In [16], task-based Functional Magnetic Resonance Imaging (fMRI) is used to investigate functional connectivity changes. They used a spatial cueing task to experiment the subjects' sustained attention during the well-rested and sleep deprived situations and using the graph theory technique, it was proved that the SD reduces the sustained attention.

1.4 Neuroimaging

1.4.1 Magnetic Resonance Imaging

Magnetic Resonance Imaging (MRI) is a medical imaging technique which uses three main components to create images of the organs of the body. As for the first part, it uses a static magnetic field created by electromagnetic coils which can be in range between 1.5 T to 7 T or higher. The second part is for transferring the energy of the desired atomic nuclei at the resonance frequency, and the third part refers to the image formation.

By altering the magnetic gradients and fluctuating electromagnetic fields, atoms inside the body can be excited. As more than 60% of the human body consists of water, there is a great amount of Hydrogen inside the body. As a result, they use the frequency of Hydrogen to tune the scanners. Hydrogen's nuclei absorbs the energy of the magnetic field. This field is used to align the protons in Hydrogen atoms in the body and using an Radio Frequency (RF) current pulsed through the patient's body, the protons will oscillate in the magnetic field and return to equilibrium. Then, the RF field is

turned off and the energy from the realignment of the protons with the magnetic field is detected by the MRI machine. The signal detected by MRI coils will be transformed into an image [21].

1.4.2 Functional Magnetic Resonance Imaging

The functions of the human brain have been always an interesting subject. Although researchers have been exploring it since many centuries ago, it is still a subject full of mysteries.

Emanuel Swedenborg was an engineer in the mid-eighteenth century who stated that each area of the brain is responsible for performing a specific task. There were other researchers who claimed the same idea before him. Scientists did not believe this idea until a few centuries later when they began examining this claim regarding the localization of functions in the brain. They could partly prove it by studying brain damage in animals or humans which gave them a better insight about the brain's organization. Nowadays, researchers use non-invasive methods such as fMRI which can be used for understanding localized functions of the brain and brain connectivity [21].

For studying the brain physiology, Ogawa and colleagues found that measuring the polarization of hydrogen was not a good method. The reason for this is that water is present throughout the body and every small change in metabolic reactions would be detected by MRI. As a result, another way was required to measure the metabolism. Ogawa suggested that oxygenated blood flow can be noticeable on T2*-weighted image of MRI. It has been found that if the molecular structure of Hemoglobin (Hb) is bound to oxygen, it would be diamagnetic. But if it is deoxygenated, it would be paramagnetic. As a result of this feature, protons near the deoxygenated Hb would have a different field strength and frequency. This makes the decay of the transverse magnetization faster. So, for the deoxygenated blood, there would be less MR signal compared to the oxygenated blood. This was an evidence that MRI can display changes in blood oxygenation [21].

While doing a certain activity, neurons in some parts of the brain become active and they need oxygen. As a result, blood flows to that area to provide more oxygen for it (Figure 1.7). The transmitted oxygen is always more than required which results in an exceed in local blood oxygen. The Blood Oxygenation Level Dependent (BOLD) is a signal which can be calculated depending on the change in oxygenation [23]. A positive BOLD signal is created when there is more neuronal activity and the signal of T2* images expand [21]. Neuronal activity which causes a rise in blood
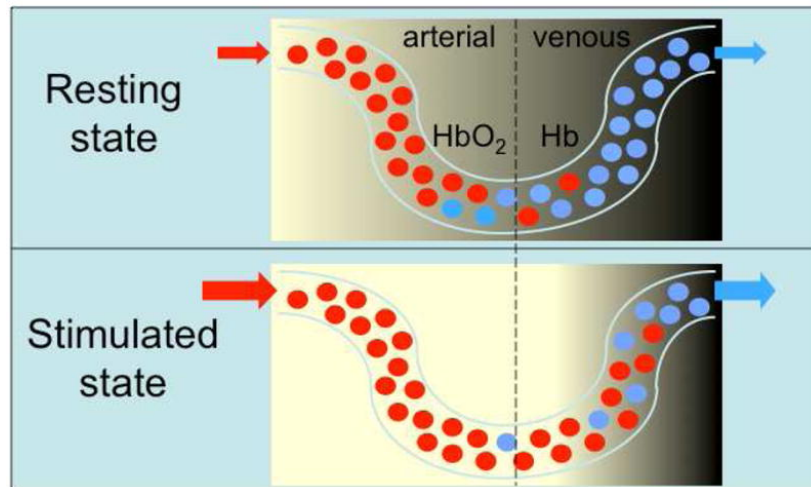
Figure 1.7: Generation of BOLD signal [22]

flow in known as the Hemodynamic Response Function (HRF) (Figure 1.8). The neuronal activity is usually very fast unlike the hemodynamic response for which it takes around 5 seconds until the blood flow reaches its maximum. Then, there is an undershoot and it takes between 15 to 20 seconds for the signal to return to the baseline [23]. Figure 1.8 part (A) shows the HRF for a short-duration event and part (B) shows the hemodynamic response to a block of multiple events [21].
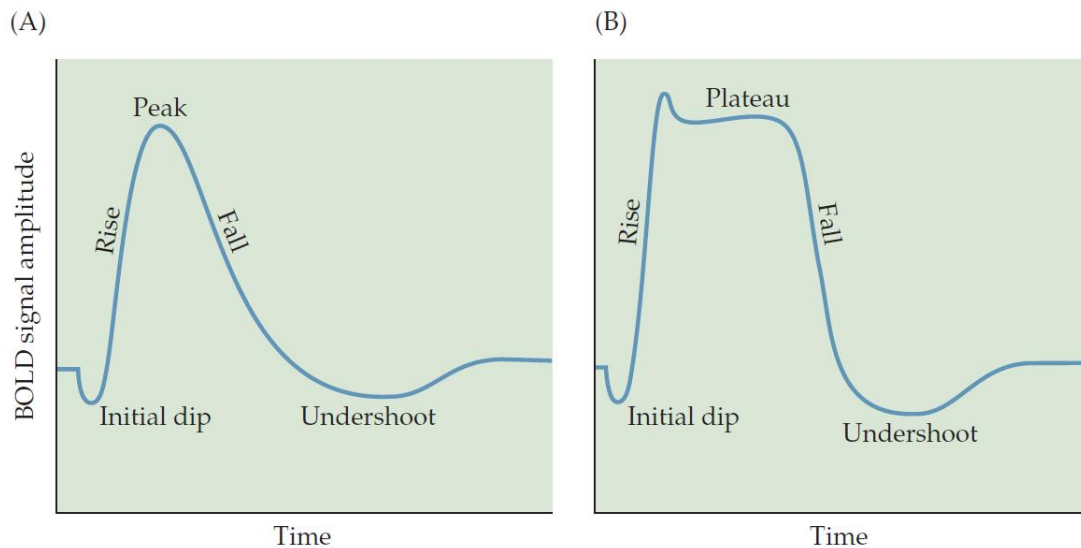
Figure 1.8: The Hemodynamic Response to (A) Single Event, (B) Multiple Events [21]

For each fMRI study, depending on the study single or multiple subjects are required. If the tasks of a study are complex, a larger sample size might be needed. Depending on the study, one or

multiple fMRI sessions can be performed and each of these sessions can contain one or more runs of functional images. There are two types of MRI images that are acquire during an fMRI session. The first one is structural MRI which shows the anatomy of the brain and its tissues. Taking one structural image with a high contrast-to-noise ratio is enough in an fMRI session. The second one is functional image which is for studying the physiology or function of the brain over time. So, in each run, multiple functional images from the brain are required which result in a time-series of volumes. The first few volumes are usually excluded from the data as the scanner might not be stable at that point. Each volume contains multiple slices of the brain which cannot be acquired simultaneously. However, all the voxels of the brain image in each slice are acquired at the same time. fMRI data analysis can be done voxel-wise or per Region-of-Interest (ROI). One can decide whether he wants to analyze each voxel of the data or divide the brain into different regions and examine functions of each region of the brain [21]. The fMRI experiment which can be used to learn more about the cognitive behaviors and activities of the brain can be performed under a Task-Based fMRI (t-fMRI) or Resting-State fMRI (rs-fMRI) condition depending on the goal of the study. In the rs-fMRI method, the experiment happens in a resting or task-negative state which means that the subjects do not perform any tasks during the MRI acquisition [24]. On the contrary, in the t-fMRI, the subjects should perform specific tasks such as finger tapping, reading, listening to a voice, looking at some pictures, playing games, etc. depending on the type of study. The reason for doing these tasks is to study the brain regions which would be activated while performing different tasks [25].

1.5   Functional Integration Studies

As explained in section 1.1, the organization of the brain consists of brain's modularity and its global function which are named as functional segregation and functional integration, respectively. These two principles should be in equilibrium so that the brain can handle its tasks. In [2], Tononi and colleagues have proposed a measure called the Neuronal Complexity or C_N which computes the interaction between functional integration and segregation. In this paper, they define functional integration and segregation using the concepts of mutual information and entropy with the assumption that the statistical properties of integration and segregation are stationary meaning that their

mean values do not change over time. Using mutual information framework, functional segregation was defined as the statistical independence of the activities of different neuronal groups, while functional integration was defined as the high level of statistical dependence of the activities between different groups. Using this new method for calculating integration and segregation, the C_N was defined which shows the effect of their interaction in a system. When both segregation and integration exist in a system, C_N is high. But when a system is completely segregated or integrated, C_N decreases [2].

In another study [26], Marrelec and colleagues extended Tononi's work and claimed that the functional integration can be measured in a hierarchical approach. They hypothesised that there are different scales in the brain such as the whole brain, brain regions and the interactions between them, and for each of these categories the integration can be calculated. So, they showed that the measure of integration can be computed for within- and between-system levels. For this aim, in an fMRI experiment, the integration was measured in six Low-Grade Glioma (LGG) patients and seven subjects as the control group. First, they consider six regions and two subsets from the fMRI data. These two subsets were defined by separating regions contralaretal to the tumor and regions ipsilateral to the tumor. Then, they calculated the total integration for the patients whole brain, between-system integration which was the integration between the two subsets, and within-system integration which was the integration within each of the subsets, and showed that the between-system integration increases in contralateral compared to ipsilateral both before and after resecting the tumor in the patients. Moreover, they proved that the integration can be measured in a hierarchical fashion [26].

In [27], Boly and colleagues showed that during NREM sleep as the consciousness decreases, functional segregation increases. In this experiment, 13 participants underwent fMRI sessions during wakefulness and NREM sleep. Using a data-driven method (independent component analysis), six networks were selected within which 77 ROIs around their local maxima was chosen. Then, a hierarchical measure of integration which was introduced in [26] was calculated between different regions of brain in both wakefulness and NREM sleep conditions. They computed the total, between-, and within-system integration at different levels such as the whole brain, brain networks, and assemblies of the areas. At the end, a new measure called Functional Clustering Ratio (FCR)

was introduced which is the ratio of the interplay of within- and between-system integration. Their results reveal that at the brain level and in each brain network, FCR increased in NREM sleep compared to wakefulness. Moreover, as both within- and between-system integrations increased during NREM sleep compared to wakefulness, total integration grew as well. In most of the networks, within-system integration increased while the results of between-system integration during NREM sleep increased, decreased or was stable in different networks. Nonetheless, the stable growth in FCR is the result of a much larger alternation in within-system integration compared to the changes in between-system integration [27].

1.6 Objectives of Thesis

One area of interest is how sleep deprivation and circadian rhythm affect functional segregation and integration. A group from University of Liège developed a study in which they examined the influence of circadian rhythm and homeostatic sleep pressure on human cognitive performance. In this sleep deprivation experiment, 33 healthy participants underwent 13 fMRI sessions during different time periods. Their aim was to study the subjects' brains responses to the sustained attention and memory performance tasks across the circadian rhythm. This study contained 42 hours of total sleep deprivation during which 12 fMRI sessions were performed, and after 12 hours of recovery sleep, the subjects underwent a 13th fMRI session. As they explored the subjects' cortical responses, it was found that the responses were changing according to the circadian rhythm although the phase was different across brain regions. Moreover, it was shown that the subcortical areas were following the melatonin profile [28].

In this thesis, we expanded the findings of our colleagues at the University of Liège and studied the effects of sleep deprivation on functional integration and segregation. We hypothesised that as the ability to learn and perform tasks decrease during sleep deprivation condition, brain's modularity or functional segregation should decrease. However, after getting enough sleep, the cellular stress would decrease which should result in an increase in functional segregation. Another goal of this project was to measure how functional integration and segregation of the brain vary with the circadian rhythm and the homeostasis sleep pressure. We wanted to check whether functional

integration follows the melatonin curve.

Moreover, in order to calculate the measure of integration, some statistical calculations must be performed which are explained in chapter 2. In [2], Tononi and colleagues explained the method for calculating the measure of integration with the assumption of having a stationary time-series. In this thesis, we decided to perform the stationarity analysis on the data to pinpoint if this stationarity assumption is actually valid. Furthermore, if any non-stationary parts were found in our analysis, we computed the measure of integration for those non-stationary along with stationary parts, and investigated the effects of this property. For this aim, the stationarity analysis was performed in small time windows for each ROI in all the subjects, and stationary and non-stationary parts of the signals were found. Afterwards, the functional integration was calculated for both stationary and non-stationary parts and it was found that more fluctuations exist in the integration results when the time-series is non-stationary compared to a stationary time-series.

The data used in this project came from the experimental procedure performed by the researchers at the University of Liège [28].

Chapter 2

Methodology

Chapter 2 discusses the definitions of time-series, auto-regressive model, and a stationary time-series. Moreover, in this chapter, we introduce a method which was used to detect stationarity in a time-series data along with an approach for computing the functional integration. Thereafter, a parameter called functional clustering ratio is explained which determines the ratio of functional segregation in a system. Finally, some comparison tests including the GLM and ANOVA are defined.

2.1   Introduction to Time-series

Time-series is a sequence of information which is acquired successively in a period of time. This information can be anything such as number of people, prices, temperature in different seasons, etc [29]. The time span that the time-series includes can be a few seconds to several years. Anyhow, a starting and ending point are essential for the time-series. If X is one observation in a time-series, a general time-series can be noted as follows.

$$\{X_t\}, t \in T \tag{1}$$

Where t is the time that each observation has occurred, and T is the entire period of the occurrence of the time-series. If X is one-dimensional, it means that only one feature of a phenomenon is used for creating the time-series model and this model is called "Univariate". On the other hand,

if several features are used in the time-series model, the model is called "Multivariate".

A time-period is the time span between two subsequent observations, and the frequency of the dataset means the frequency that the observations occur. For analyzing the data effectively, it is better to know at what time or how often the observations are happening. The values in a time-series usually depend on time, and the past values as well as other exterior factors which influence the current values. So, each time-series has a certain behavior and using its previous behavior, the future values of the time-series can be forecasted with some approximations [29, 30, 31]. In most cases, the mean and the covariance of a time series can be written as follows.

$$\mu_t = E(X_t) \tag{2}$$

$$COV(X_t, X_s) = E[(X_t - \mu_t)(X_s - \mu_s)] \tag{3}$$

Where $E(X_t)$ is the expected value or mean of X_t, and t and s are the time points for two different observations. The mean and the covariance of a time-series can depend on the time if the time-series is non-stationary or be independent of the time in case of a stationary time-series. The notion of stationarity is explained in section 2.3. As mentioned, different values in a time-series are correlated to each other and for understanding the pattern of these correlations, statistical modelling can be used if the series is stationary and it follows a linear model. So, the properties of the time series should remain constant and as a result, the series can be represented using a linear model of their past and present values [30, 32].

2.2 Auto-Regressive Model

As mentioned in the previous section, a time-series is a sequence of information from a variable over time. A model which regresses values of a time-series on its past values is called an Auto-Regressive (AR) model [33]. It means that the present value of the time-series linearly depends on its past values or in other words, the past values of a time-series along with a random shock can explain its present value [29, 30]. The following equation represents the AR model.

$$y_t = \beta_0 + \beta_1 y_{t-1} + \varepsilon_t \qquad (4)$$

In equation (4), y_t is the current value, y_{t-1} is the past value, β_0 is a constant value, β_1 is the parameter of the model and ε_0 is the white noise in this regression model. In the AR model, y_{t-1} is the predictor of the current value. An important factor in AR model is its order which is the number of previous values that would be used in order to predict the present value. So, the model shown in equation (4) is called a First-order AR (AR(1)) model. The Second-order AR (AR(2)) model which predicts the present value from the values of times $t-1$ and $t-2$ can be written as follows.

$$y_t = \beta_0 + \beta_1 y_{t-1} + \beta_2 y_{t-2} + \varepsilon_t \qquad (5)$$

y_{t-2} is the second previous value. This second-order AR model can be written as AR(2). In the same sense, the kth-order AR or AR(k) is a model which predicts the present value from the values at times $t-1, t-2, ..., t-k$. y_t is a dependent variable as its value depends on the values of $y_{t-1}, y_{t-2}, ..., y_{t-k}$ which are the independent variables [29, 30, 33].

2.3 Stationary Time-series

In a time-series data, a regularity in its behavior over time might be seen. This regularity can be explained by the notion of a stationary process [30]. There exist different notions of the stationary processes. A time-series is considered strong-sense or strict-sense stationary when the statistical properties of the time-series are shift-invariant which means that they do not depend on time. So, the process $X = \{x_i; i \in Z\}$ is strictly stationary if:

$$F_X(x_{t_1}, ..., x_{t_n}) = F_X(x_{t_{1+\tau}}, ..., x_{t_{n+\tau}}) \qquad (6)$$

$t_1, t_2, ..., t_n$ are all the time points and τ is the shift which can be $\tau = 0, \pm 1, \pm 2, ...$ In practice, a strict-sense stationary condition rarely happens [29, 30].

A time-series is called Weak-Sense Stationary (WSS) if it has a finite variance, its mean value is constant and shift-invariant, and its auto-covariance function depends only on a time difference

17

$s - t$. Weak-sense stationary process has less restrictive requirements compared to the strict-sense stationary [29, 30]. In this thesis for simplicity, we use the term stationary to refer to a weakly stationary time-series. So, the process $X = \{x_i; i \in Z\}$ is WSS if:

$$\forall t, E[x_i] = \mu \tag{7}$$

$$\forall t, var[x_t] < \infty \tag{8}$$

$$\forall (s,t), \gamma(s,t) = COV(x_s, x_t) = E[(X_s - \mu_s)(X_t - \mu_t)] \tag{9}$$

These conditions mean that the mean is constant (Equation 7), the variance is constant and finite (Equation 8), and the auto-covariance only depends on $|s - t|$ for all time points s and t (Equation 9) [29, 30]. Figure 2.1 shows stationary versus non-stationary time-series.
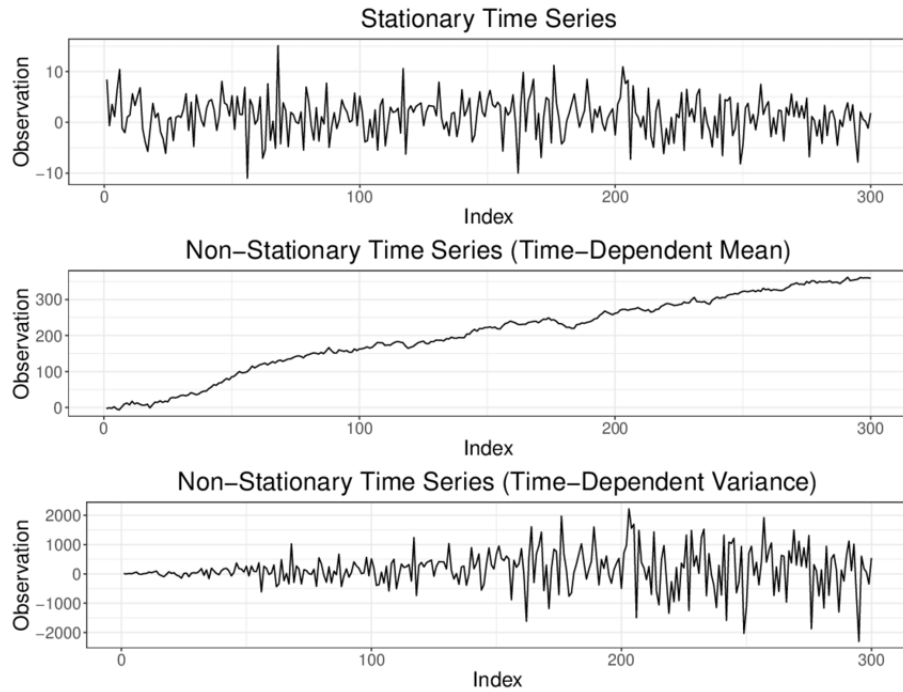
Figure 2.1: Stationary versus non-stationary time-series [34]

A time-series is Trend-stationary when the model fluctuates around a deterministic trend. This can be a linear or quadratic trend but the amplitudes of oscillations around this trend remain similar over time. If this trend can be removed, the signal becomes stationary [35].

One of the most important features of a stationary process is that shocks do not have a long effect on them. Shocks temporary effect on a stationary time-series disappears over time and the time-series would return to its long-term mean level [36]. There are several different statistical methods with which one can determine if a signal is stationary or not. Some of these methods are explained in section 2.4.

2.4 Detecting Stationarity in Time-series

There are numerous parametric tests such as the unit root tests for detecting stationarity in the time-series data [37]. In the unit root tests method, if a unit root is found in a time-series, it means that it is not stationary as it would have an unpredictable pattern. As a result, the null hypothesis (Equation 10) is that there exists a unit root which makes the time-series non-stationary, and the aim is to reject this hypothesis with a high level of confidence and accept the alternative hypothesis (Equation 11) [29, 30, 38].

$$H_0 : \beta = 1 \tag{10}$$

$$H_1 : |\beta| < 1 \tag{11}$$

Two of the unit root tests are explained in sections 2.4.1 and 2.4.2.

2.4.1 The Dickey-Fuller Test

This test that was created by two statisticians, David Dickey and Wayne Fuller, analyzes an auto-regressive time-series model with a Least-Square (LS) estimator to determine if there are any irregular patterns in the data and the null hypothesis can be accepted or rejected. In the Dickey-Fuller (DF) test, the first lag of AR model or AR(1) was used. If we consider the AR(1) as $y_t = \beta y_{t-1} + \varepsilon_t$ for $t = 1, 2, ..., n$ and no constant term, the LS estimator of β can be written as:

$$\hat{\beta} = \frac{\sum_{t=2}^{n} y_{t-1} y_t}{\sum_{t=2}^{n} y_{t-1}^2} = \beta + \frac{\sum_{t=2}^{n} y_{t-1} \varepsilon_t}{\sum_{t=2}^{n} y_{t-1}^2} \tag{12}$$

In equation (12), the ˆ sign above the coefficient means a LS estimator [39]. In this equation,

when the time-series is stationary meaning that $|\beta| < 1$, the sequence of $n^{\frac{1}{2}}(\hat{\beta} - \beta)$ would have a normal distribution of $N(0, 1 - \beta^2)$. But when $\beta = 1$ meaning that the time-series in non-stationary, both the numerator and the denominator would have a non-normal distribution [29, 39]. For generating the DF model, first we subtract the y_{t-1} term from both sides of AR(1) model. As a result, the testing hypothesis would change to $\delta = 0$ and δ can be defined as $\delta = \beta - 1$ [36]. The DF model has three versions which are as follows.

$$\Delta y_t = \delta y_{t-1} + \varepsilon_t \tag{13}$$

$$\Delta y_t = a_0 + \delta y_{t-1} + \varepsilon_t \tag{14}$$

$$\Delta y_t = a_0 + a_1 t + \delta y_{t-1} + \varepsilon_t \tag{15}$$

The first formula is a pure random walk process while the second model considers a drift or intercept term (a_0), and the last model considers both a drift and a deterministic time trend ($a_1 t$) [36].

As mentioned, the DF test uses the first lag of AR model and it cannot be a good analysis method for time-series with more complicated structures. The more complicated versions of this test are the Augmented Dickey-Fuller (ADF) and the Phillips-Perron (PP) [36].

2.4.2 The Augmented Dickey-Fuller Test

If a time-series is complicated and has serial correlations, the powerful ADF test can be used to determine if it is stationary. The ADF test uses higher order AR models, AR(1+p). Like section 2.4.1, for the ADF test, we should test if $\delta = 0$ where $\delta = \beta - 1$ to determine if the data is non-stationary [29]. Like the DF test, the ADF test has three versions; the first one does not have a constant or trend, the second one uses a constant, and the third one includes a constant and a trend. The difference between DF and ADF is that in the latter, p which is the order of the AR model or the lagged differences are added in the model [30, 36, 40].

$$\Delta y_t = \delta y_{t-1} + \sum_{s=1}^{p} a_s \Delta y_{t-s} + \varepsilon_t \tag{16}$$

$$\Delta y_t = a_0 + \delta y_{t-1} + \sum_{s=1}^{p} a_s \Delta y_{t-s} + \varepsilon_t \tag{17}$$

$$\Delta y_t = a_0 + a_1 t + \delta y_{t-1} + \sum_{s=1}^{p} a_s \Delta y_{t-s} + \varepsilon_t \tag{18}$$

2.5 Calculating the Measure of Integration

In order to calculate the measure of functional integration, Tononi and colleagues [2] have used mutual information and entropy which are concepts defined in the information theory. These two measures can be used together to calculate the level of the statistical dependence in a time-series data [2, 26].

Consider y as a Gaussian distributed random variable which possesses a mean of $\mu = \mu_n$ and a covariance matrix of $\Sigma = \Sigma_{n \times n}$ where $n = 1, 2, ..., N$, and N is the regions associated with a fMRI time-series [26]. The entropy of y can be defined as:

$$H[p(y)] = -\int p(y) ln(p(y)) dy \tag{19}$$

$$H[p(y)] = \frac{1}{2} \ln[(2\pi e)^N |\Sigma|] \tag{20}$$

In equation (19), $p(y)$ is the probability distribution of y. In equation (20), $|.|$ stands for the determinant and this equation shows the joint entropy of y which, as mentioned, is a Gaussian distributed random variable. Entropy shows the level of uncertainty [1] or randomness in a system. It is positive definite and when the probability is equal to 1, the entropy is always zero.

The relative entropy or the Kullback–Leibler (KL) divergence shows how two probability distributions are different from each other. The KL divergence between two probability distributions $p_1(y)$ and $p_2(y)$ is [26]:

$$D_{KL}[p_1(y); p_2(y)] = \int p_1(y) ln \frac{p_1(y)}{p_2(y)} dy \tag{21}$$

If $p_1(y)$ and $p_2(y)$ are similar, the D_{KL} is zero. For calculating the level of dependence for a

partition of a system, mutual information or KL information proper can be used. For this aim, the KL method should be measured between the marginal and joint distributions of that system [26]. The formula is as follows.

$$MI[y_1, ..., y_k] = D_{KL}[p(y_1, ..., y_k); \prod_{k=1}^{K} p(y_k)] \tag{22}$$

In this equation, MI stands for the mutual information. In [26], they showed that equation (22) can be written as follows.

$$MI[y_1, ..., y_k] = [\sum_{k=1}^{K} H[p(y_k)]] - H[p(y_1, ..., y_K)] \tag{23}$$

When two partitions are independent from each other, the sum of their entropies is maximal, and the mutual information or D_{KL} is zero. But if they share some properties and depend on each other, their entropy is decreased, and the mutual information would be a positive value [2, 26].

Mutual information can be measured for a one-dimensional component such as a brain region and this measure is called the integration as explained in [2]. Total integration, which is the interactions between different areas in the brain, is calculated by the difference between the sum of entropies of all individual components (y_k) in a system considered independently while excluding the entropy of the entire system ($y_1, ..., y_k$) [2, 26].

$$I[y_1, ..., y_k] = [\sum_{k=1}^{K} H[p(y_k)]] - H[p(y_1, ..., y_k)] \tag{24}$$

Considering that y is a Gaussian distributed random variable, the previous equation can be written as:

$$I[y_1, ..., y_k] = \frac{1}{2} \ln[\frac{\prod_{n=1}^{N} \Sigma_{n,n}}{|\Sigma|}] \tag{25}$$

The measure of integration can be calculated for different levels of the brain as suggested in [26]. This means that the integration within a specific network or between different networks or the total integration for the whole brain can be measured. The Σ in equation (25) can be defined as:

$$\Sigma = [diag(\Sigma)]^{\frac{1}{2}} \mathcal{R} [diag(\Sigma)]^{\frac{1}{2}} \tag{26}$$

Where $\mathcal{R}$ corresponds to the correlation matrix and $diag(\Sigma)$ is the values which are on the diagonal of the variance matrix.

The integration within a system can be calculated as follows.

$$I_{ws} = I[(y_n)_{n \epsilon \mathcal{S}_k}] = [\sum_{n \epsilon \mathcal{S}_k} H[p(y_n)] - H[p(y_{\mathcal{S}_k})]] \tag{27}$$

$$I_{ws} = \frac{1}{2} \ln[\frac{\prod_{n \epsilon \mathcal{S}_k} \Sigma_{n,n}}{|\Sigma_{\mathcal{S}_k, \mathcal{S}_k}|}] \tag{28}$$

Where n represents each region which exist within a chosen system, and $\mathcal{S}_k$ is the intended system and in equation (28), $|\Sigma_{\mathcal{S}_k, \mathcal{S}_k}|$ is the covariance matrix associated with $y_{\mathcal{S}_k}$. The integration between different systems is defined as:

$$I_{bs} = I[y_{\mathcal{S}_1}, ..., y_{\mathcal{S}_k}] = [\sum_{k=1}^{K} H[p(y_{\mathcal{S}k})] - H[p(y_{\mathcal{S}_1}, ..., y_{\mathcal{S}_k})]] \tag{29}$$

$$I_{bs} = \frac{1}{2} \ln[\frac{\prod_{k=1}^{K} |\Sigma_{\mathcal{S}_k, \mathcal{S}_k}|}{|\Sigma|}] \tag{30}$$

Where K is the number of desired subsets. It can be shown that the total integration can be measured using the within-system and between-system integrations. For a network with K subsets, the total integration is defined as [26]:

$$I_{tot} = I_{bs} + \sum_{k=1}^{K} I_k \tag{31}$$

On a global scale, the measure of integration shows how much statistical dependency exists in a system. Thus, integration links to how integrated the functional brain networks are. All the equations presented in this section are explained in [26] in which the hierarchical measure of integration was first introduced.

2.6 Functional Clustering Ratio

FCR as defined in [27] is a measure for determining the ratio of functional segregation in a system. For this aim, the integration within a subsystem should be divided by the integration between the subsystems. If the value of FCR is high, it means that there is not much functional dependency between the subsystems and the functional segregation increases.

$$FCR = \frac{I_{ws}}{I_{bs}} \tag{32}$$

In [27], the value of FCR is compared between wakefulness and NREM sleep. For this aim, they calculated the total, within- and between-system integration of the whole brain and networks, and measured FCR afterwards. For example, in order to calculate FCR between the whole brain and the networks, the integration within the brain and the integration between six chosen networks shown in figure were measured. Then, using the formula, they calculated the FCR for wakefulness and NREM sleep. Their results prove that FCR value increases during NREM sleep comparing to the wakefulness. There was also an increase in total integration as well as both within- and between-network integration during NREM sleep compared to wakefulness.
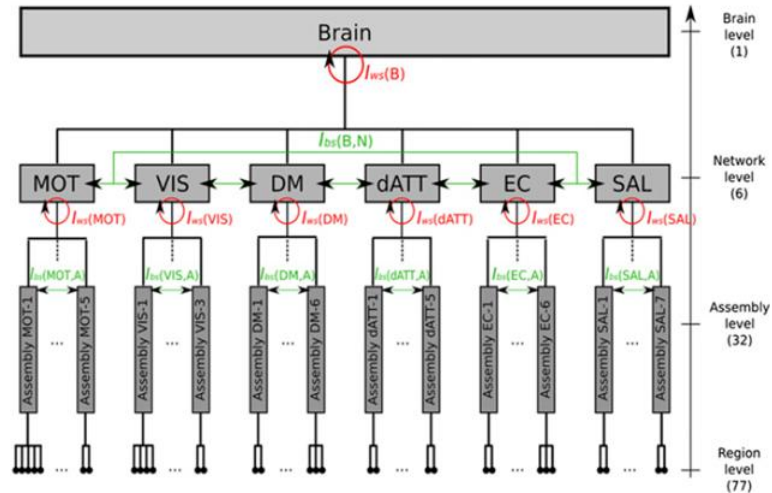
Figure 2.2: Levels of hierarchical integration in the brain [27]

2.7 Sliding Window Approach

In this thesis, we calculated all the parameters including the stationarity, measure of integration, and FCR within a sliding window.

In the sliding window technique, a window with a fixed size is chosen, it moves through the data and in each of the moving windows, some statistics would be calculated. The window keeps sliding and some computations would be performed window by window until all the data is covered. One of the parameters that can be defined in this method is the overlap length. Using this parameter, it can be determined whether the current window can have an overlap with the previous window [41]. In this approach, finding a suitable window size is an essential factor.
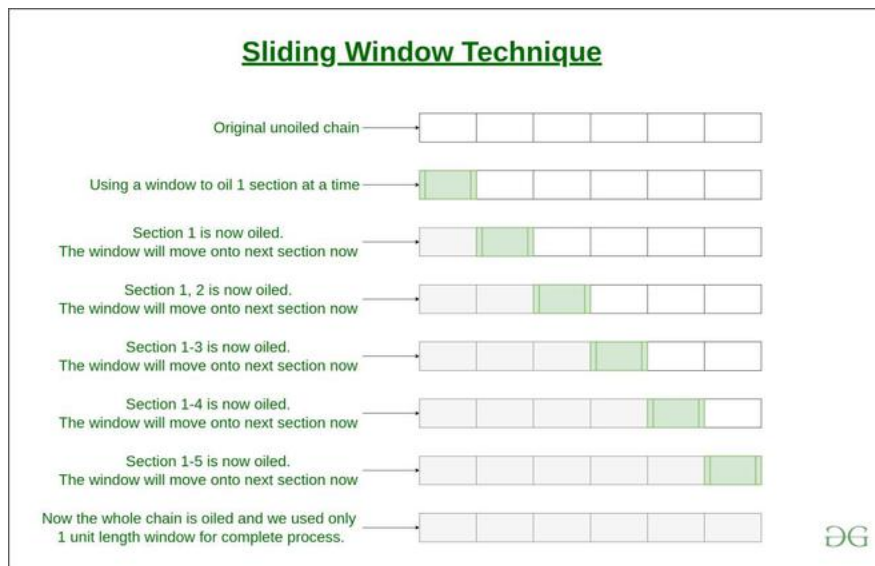
Figure 2.3: Sliding Window Technique [42]

In this thesis, in order to find periods of stationarity in the given time-series data, it is necessary to partition the series into smaller samples. Starting from the beginning of the series, Unit Root test is conducted on samples within a window, then the windows is shifted to the following slides. As mentioned, neighboring windows can overlap and contain shared samples between each other. The number of shared samples can be adjusted.

2.8 The Generalized Linear Model

The Generalized Linear Model (GLM) is a statistical analysis framework which relates some predictors to an outcome using linear or logistic regression. GLM is the basis of many statistical tests such as ANOVA, ANCOVA and regression analysis. Most of these tests fit the definition of $Data = Model + Error$. Using the linear regression form of the GLM, some linear predictors with their coefficients like $X\beta = \beta_0 + X_1\beta_1 + ... + X_k\beta_k$ can be defined and the outcome, y, would be determined using one or more predictors. Moreover, a link function g is also used for modeling the data $\hat{y} = g^{-1}(X\beta)$ [43].

Linear regression methods try to find a linear relationship between the predictors and the output. Their output always has a normal distribution with mean μ. However, in GLM, the output can have a normal, binomial, poisson, gamma, or inverse Gaussian distribution [44].

2.9 The ANOVA Test

ANOVA which stands for Analysis of Variance was first introduced by Ronald Fisher. Analysis of Variance (ANOVA) uses variances of independent groups to determine if they possess different mean scores. Two most common types of this test are One-Way and Two-Way ANOVA which are defined by the number of independent variables they contain. One-way or single factor ANOVA includes one independent variable, while two-way ANOVA is a test that considers two independent variables [45].

One-way ANOVA which uses a simple linear model can be writen as:

$$y_{ij} = \alpha_j + \varepsilon_{ij} \tag{33}$$

Where i is the observation number, j is the group number, y_{ij} is an observation, α_j is the group's mean and ε_{ij} is the error. The null hypothesis in one-way ANOVA is that the means of all the groups are similar ($H_0 : \alpha_0 = \alpha_1 = ... = \alpha_k$), while the alternative hypothesis is that group means can be different ($H_1 : \alpha_i \neq \alpha_j$ at the minimum for one group) [46].

In two-way ANOVA, the test is performed on a desired variable to determine if two different

factors whether they have any interactions or not have any influence on that variable. The model for the two-way ANOVA is as follows [47].

$$y_{ijr} = \mu + \alpha_i + \beta_j + (\alpha\beta)_{ij} + \varepsilon_{ijr} \tag{34}$$

Where i is the group's row, j is the group's column, r is an independent observation or replication number, y_{ijr} is an observation, μ is the mean, α_i is the effect of the $i-th$ row factor, β_j is the effect of the $j-th$ column factor, $(\alpha\beta)_{ij}$ is any interaction between the $i-th$ row and the $j-th$ column factors, and ε_{ijr} is the error.

The null- and alternative-hypothesis in the two-way ANOVA are as follows.

(1) The first null-hypothesis is that the means of the row factors are equal ($H_0 : \alpha_0 = \alpha_1 = ... = \alpha_I$), while the alternative hypothesis is that at least one mean is different ($H_1 : at\ least\ one\ \alpha_i\ is\ different,\ i = 1, 2, ..., I$).

(2) The second null-hypothesis is that the means of the column factors are equal ($H_0 : \beta_0 = \beta_1 = ... = \beta_J$), while the alternative hypothesis is that at least one mean is different ($H_1 : at\ least\ one\ \beta_j\ is\ different,\ j = 1, 2, ..., J$).

(3) The third null-hypothesis is that there is no interactions between the row and column factors ($H_0 : (\alpha\beta)_{ij} = 0$), while the alternative hypothesis is that at the minimum there is interaction between one row and column factor ($H_1 : at\ least\ one\ (\alpha\beta)_{ij} \neq 0$) [47].

Chapter 3

Study Design

Chapter 3 provides a complete description on the criterion to choose the participants, study design, the tasks performed in the MRI scanner, a summary of the data acquisition procedure and the data preprocessing steps. At the end, an atlas called MIST which was used in this thesis is explained.

Hiring the participants, the data acquisition and the preprocessing of fMRI data were done in the Faculty of Medicine of the University of Liège after the experiment was approved by their Ethics committee. The procedure of the data acquisition for this study was explained completely in [48].

3.1 Participants

36 healthy, right-handed subjects were chosen who signed a consent form to be included in the study and they were remunerated. The criterion for choosing these 36 subjects from a large group of people was as follows. They were not consuming any medication or psychoactive drugs, and moderate consumption of caffeine ($<$ 3 cups per day) and alcohol ($<$ 7 units a week) was permitted. Also, it was determined that the subjects did not suffer from any medical, traumatic, psychiatric or sleep disorders by undergoing semi-structured interviews. Another important factor in this study was the absence of a poor sleep quality. Using the Pittsburgh Sleep Quality Index (PSQI) which is a self-rated questionnaire [49], the quality of the subjects' sleep was measured and 5 people were excluded. Also, using the Epworth Sleepiness Scale (ESS) which is also a self-rated

questionnaire [50], the excessive daytime sleepiness was measured and 10 people were excluded at this level. The other exclusion criteria were extreme chronotype, having night shifts during the foregoing year, travelling to more than one time region in the previous three months and the body mass which had to be more than 27 $\frac{kg}{m^2}$. With respect to these criterion, 36 subjects were chosen, but later three of them were excluded from the study as their melatonin data was not complete [48].

3.2 Protocol

For this experiment, the subjects had to assess their sleep timing at home three weeks prior to going to the laboratory. During the last week of this self-assessment, each individual had to choose a sleep timing between 0:00 – 8:00 and 1:00 – 9:00. They had to follow the sleep timing which was closest to their habitual sleep cycle. These new schedules were on average 18 minutes different from the individuals' sleeping times and 8 minutes different from their waking times [48]. In this thesis, the participants who chose the first schedule are called the "Morning Group" and the ones who chose the second schedule are called the "Evening Group".
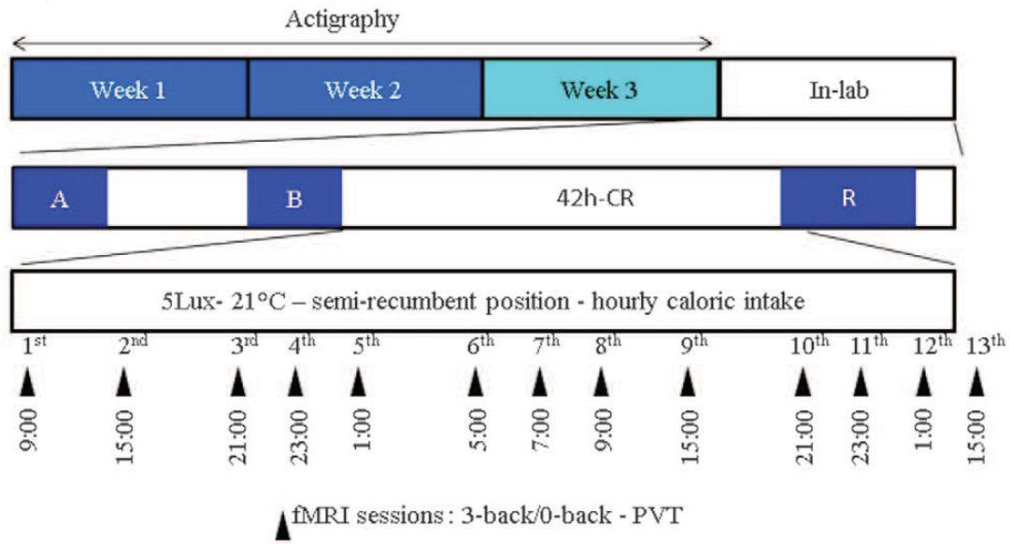
Figure 3.1: The study protocol [28]

Afterwards, they had to stay in the lab for 4 days to learn the protocol and undergo the fMRI data acquisition. On the first day in the lab, the subjects learned more about the tasks they had to

do in the MR scanner, structural MR scans were acquired, and urine test was done to be analyzed for the drugs. During the first night (labeled "A" in Figure 4.1), which is called the adaptation night, in order to detect sleep disorders such as sleep related breathing disorders or periodic limb movements a full Polysomnography (PSG) was recorded [48]. The PSG is a sleep study that is used for detecting sleep disorders [51].

The next day, for assessing the daytime need for sleep, five sleep latency tests were performed. The second night of sleep was a baseline night in which the PSG was recorded (labelled "B" in Figure 4.1). During these two nights, the subjects slept according to the sleep schedule which they chose before (0:00 – 8:00 or 1:00 – 9:00) [48].

After waking up from the baseline night, the main part of the study began. The subjects were put in individual, soundproof rooms in which the light, temperature and humidity could be controlled. Also, they were under constant Closed-Circuit Television (CCTV) and EEG monitoring. The data acquisition consisted of 12 fMRI sessions which were performed across a 42-hour constant sleep deprivation and a last fMRI session was done after a 12-hour recovery sleep on 33 healthy subjects. During the 42 hours of SD, they had a Constant Routine (CR) and for melatonin measurements, every hour salivary samples were taken (Figure 3.2).
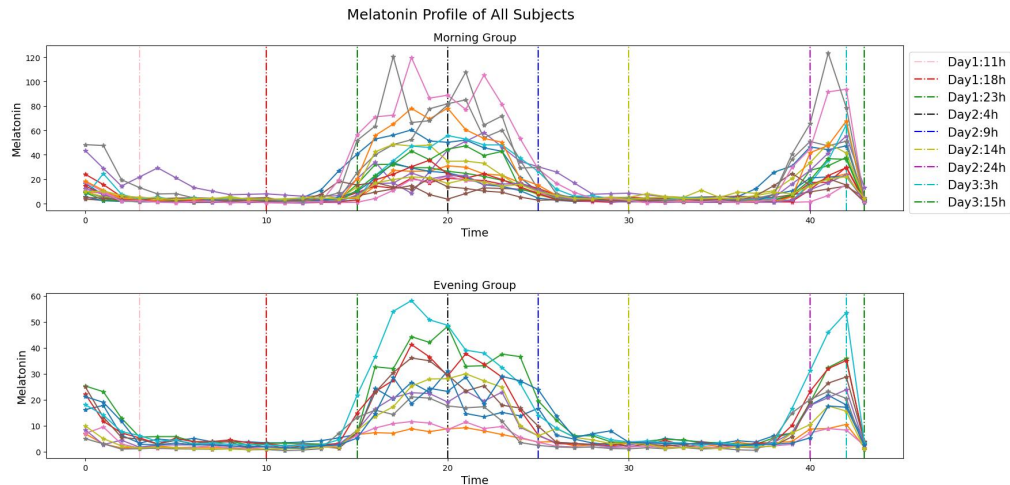
Figure 3.2: Melatonin Profile of All Subjects

The twelve fMRI sessions during the SD period were scheduled at specific times of the day, evening, and night. For the morning group, the scans schedule was 9:00, 15:00, 21:00, 23:00, 01:00,

30

5:00, 7:00, 9:00, 15:00, 21:00, 23:00, 01:00, and for the evening group, it was one hour after the morning people's sessions. Karolinska Sleepiness Scale (KSS) was recorded thirty minutes before each fMRI session. During each fMRI session, subjects performed two tasks. The first run was an auditory 3-back or 0-back task which were randomly performed, and the second run included a Psychomotor Vigilance Task (PVT) session [48].

During the 12-hour recovery sleep which started at the end of the 12th fMRI session, the subjects had to stay in the bed and the lights were off until the end of the 12 hours period. On the last day, an hour after waking up from the recovery sleep, the last (thirteenth) fMRI session was acquired and a waking EEG was recorded [48].

3.3 Tasks Description

3.3.1 The Psychomotor Vigilance Task

The PVT is a reaction time task which measures how regular the subjects respond to a stimulus. It simply measures the sustained attention in each individual and this task is commonly used for studies which are related to sleep dept. The reason for this is that as the period of sleep deprivation increases, it is harder for the subjects to keep alert and respond correctly to the tasks as a result of reduced psychomotor skills [52].

In this experiment, during the PVT session, subjects had to look constantly at a cross on a black screen. This cross was changed at a random timing of 2 to 10 seconds and a scrolling millisecond counter would appear instead. The participants had to press a button to stop the counter as soon as possible. The duration of this task was 10 minutes [48].

3.3.2 The N-Back Task

In cognitive neuroscience, N-Back task which was introduced by Wayne Kirchner [53] is used for measuring the performance and the working memory [54].

In this study, 4 blocks of 0-back and 6 blocks of 3-back tasks were chosen which were generated in random and there were 10 to 20 seconds of resting periods in between the runs. Also, no more than two consecutive blocks could be similar. In each block, the subjects were instructed to listen to

30 consonants which were presented in 2 seconds. In case of 3-back blocks, they had to press a key to determine if the current letter was identical to the letter of three stimuli before, while in 0-back task, they had to press a key in case of hearing the letter "K". The duration of this task was 15 minutes. The data of 2 subjects was discarded from the N-Back analysis as they showed a learning curve [48].

3.4 MRI Data Acquisition

The MRI scans were acquired using a 3T head-only scanner. The scanner's settings for acquiring the high-resolution T1-weighted or structural images were as follows; 3D MDEFT; $TR = 7.92ms$, $TE = 2.4ms$, $TI = 910ms$, $FA = 15°$, $FoV = 256 \times 224 \times 176mm^3$ and $1mm$ isotropic spatial resolution. Also, for obtaining the multislice T2*-weighted or functional images, a gradient-echo Echo-Planar Imaging (EPI) sequence was used which has axial slice orientation and covers all of the brain. The settings for the T2*-weighted images are as follows; 34 slices, $FoV = 192 \times 192mm^2$, voxel size $3 \times 3 \times 3mm^3$, 25% interslice gap, matrix size $64 \times 64 \times 34$, $TR = 2040ms$, $TE = 30ms$ and $FA = 90°$.

During the N-back session, approximately 360 to 390 functional images, while during the PVT session, about 300 to 315 images were obtained and in both of these sessions, the first three volumes were dropped from further processing to compensate for the saturation effect of the T1 scan. A screen was placed at the end of the scanner with which the stimuli was shown and through a mirror which was on the standard head coil, the subjects could see the displayed stimuli.

3.5 The fMRI Data Preprocessing

The data preprocessing was done at the university of Liège and they did it using Statistical Parametric Mapping (SPM) (SPM8) which was executed through MATLAB.

The motion and distortion correction using Realign and Unwarp was used for the EPI time-series. First, the realignment which is for motion correction was performed for the images of all the subjects. Then, the mean EPI image was spatially coregistered to the structural images and the coregistration parameters were used for the BOLD time-series realignment. After that, the

spatial normalization into the Montreal Neurological Institute (MNI) space was performed for each anatomical scan and a unified segmentation approach was used. Using the estimated warping, the normalization for the functional images was then performed and using a Gaussian kernel of $8mm$ Full Width at Half Maximum (FWHM), they were smoothed spatially.

3.6 MIST Atlas

In functional connectivity studies, analysing just one voxel is not very resourceful. The best way to practice functional connectivity is using brain parcellations which display the interactions within the whole-brain. There are several brain atlases which can be used to perform the brain parcellation. In this thesis, we used the Multiresolution Intrinsic Segmentation Template (MIST) atlas. MIST as defined in [55] is a brain atlas with which brain's cortical, subcortical and cerebellar gray matter can be parcelled into multiple resolution groups. Using this atlas, functional brain networks can be parcelled in MNI152 space into nine different spatial resolutions from 7 large networks to 444 individual functional areas [55].

One of the main goals for creating MIST was to follow how functional networks split into smaller areas, and for this goal, they used Multiscale Stepwise Selection Algorithm (MSTEPS) to pinpoint these nine resolutions (4, 12, 20, 36, 64, 122, 197, 325, and 444) which are shown in Figure 3.3. They also generated a parcellation of resolution 210 from parcels of resolution 122, and named it the ROI resolution [55].

The reason we decided to use this atlas was that it would give us flexibility to choose with which parcellation we wanted to work, and we had the chance to use multiple resolutions and compare the results. In this thesis, the MIST atlas with 64, 122, and 210 parcellations was used to extract the regional BOLD time-series. Although we worked with all three resolutions for the stationarity and integration analysis which are explained in the next chapter, we decided to keep our focus on MIST64. As we were using the sliding window method to compute the stationarity and measure of integration, having less columns in our fMRI time-series matrix was more beneficial for us. One of our restrictions which is explained thoroughly in section 4.1 of the next chapter was that the number of columns had to be equal or less than the number of columns.
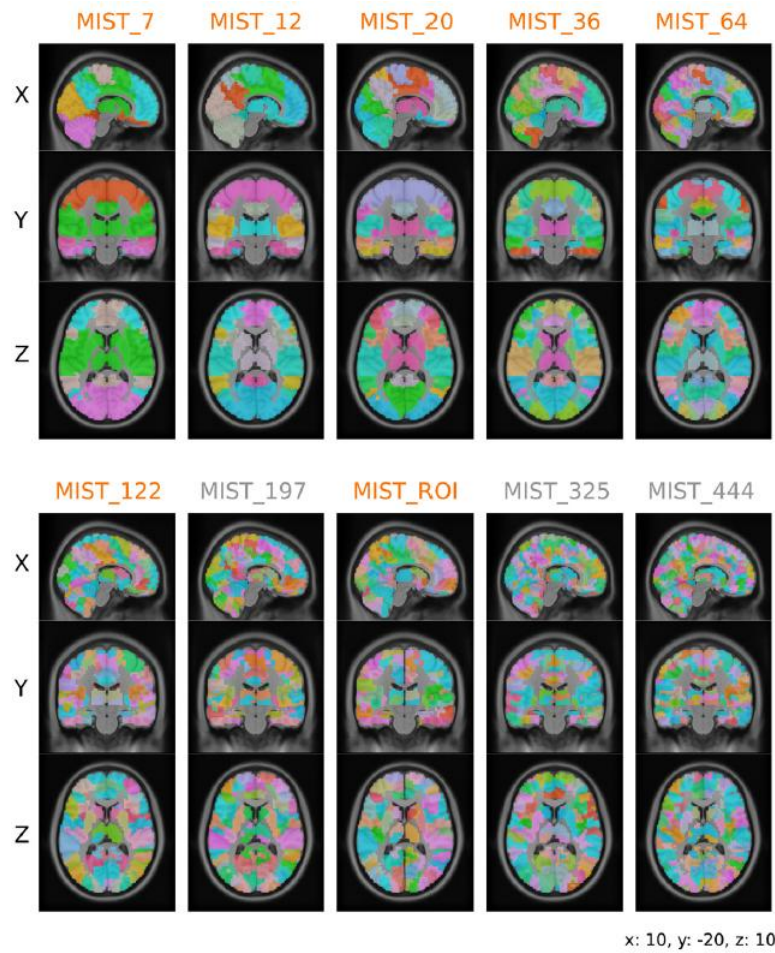
Figure 3.3: MIST Atlas Parcellation Overview

Chapter 4

Results

In this chapter, we first look into the results of the stationarity analysis. In section 4.1, the stationarity analysis was performed for different sliding window sizes, overlaps, and distinct properties for the ADF test. After choosing the proper properties for our model, we move forward to section 4.2 to compute the measure of integration for both non-stationary and stationary parts of the data in order to determine the effects of stationarity in our analysis. Afterwards, the FCR is calculated for wakefulness and SD conditions. At the end, we explore the results of GLM and ANOVA tests.

First, using the MIST atlas the regional BOLD time-series for all the subjects was extracted from the 4-D fMRI dataset. As mentioned in the previous chapter, the MIST atlas has different resolutions. In this thesis, the MIST atlas with the resolution of 64 is used. After extracting the regional BOLD time-series, the first step was to preprocess the data. This step involved searching for any missing data, cleaning them and normalizing the data.

In order to correct the missing or Not a Number (NaN) values which were found in the time-series, the average of the neighbors method was used. In this method, the NaN value would be replaced by the average of its previous and next neighbors. After cleansing the data, it was normalized using the min-max method which is as follows.

$$X' = \frac{X - X_{min}}{X_{max} - X_{min}} \tag{35}$$

Using this method, all the values in each time-series was scaled to be between zero and one.

35

This way, the minimum value for all the time-series would be transformed to 0, and its maximum would be changed to 1.

4.1 FMRI Time-series Stationarity

In this thesis, the stationarity analysis was performed on the fMRI time-series data of 27 subjects each of which underwent 13 fMRI sessions containing N-back and PVT sessions. 6 out of 33 subjects were excluded from the analysis due to incomplete fMRI sessions or incomplete melatonin profiles.

To calculate the stationarity of the time-series, the "adftest" function from MATLAB's Econometrics Toolbox was used which is the Augmented Dickey-Fuller test. The main parameters in this test are the type of the model, the order of the AR model, alpha or the nominal significance level for the hypothesis test and the test statistic.

In MATLAB, the type of the model can be selected as either AR, Autoregressive model with Drift variant (ARD) or Trend-Stationary model variant (TS). In AR model, like the equation (16), a simple AR model is used. In ARD model, like the equation (17), a potential drift for the time-series is also taken into account in the stationarity analysis, and in TS model, like the equation (18), a potential trend for the time-series is considered. The details for each of these models are as follows.

Model Variant Name	Description
"AR"	Autoregressive model variant, which specifies a test of the null model $$y_t = y_{t-1} + \beta_1 \Delta y_{t-1} + \beta_2 \Delta y_{t-2} + \ldots + \beta_p \Delta y_{t-p} + \varepsilon_t$$ against the alternative model $$y_t = \phi y_{t-1} + \beta_1 \Delta y_{t-1} + \beta_2 \Delta y_{t-2} + \ldots + \beta_p \Delta y_{t-p} + \varepsilon_t,$$ with AR(1) coefficient $\phi < 1$.
"ARD"	Autoregressive model with drift variant, which specifies a test of the null model $$y_t = y_{t-1} + \beta_1 \Delta y_{t-1} + \beta_2 \Delta y_{t-2} + \ldots + \beta_p \Delta y_{t-p} + \varepsilon_t$$ against the alternative model $$y_t = c + \phi y_{t-1} + \beta_1 \Delta y_{t-1} + \beta_2 \Delta y_{t-2} + \ldots + \beta_p \Delta y_{t-p} + \varepsilon_t,$$ with drift coefficient c and AR(1) coefficient $\phi < 1$.
"TS"	Trend-stationary model variant, which specifies a test of the null model $$y_t = c + y_{t-1} + \beta_1 \Delta y_{t-1} + \beta_2 \Delta y_{t-2} + \ldots + \beta_p \Delta y_{t-p} + \varepsilon_t$$ against the alternative model $$y_t = c + \delta t + \phi y_{t-1} + \beta_1 \Delta y_{t-1} + \beta_2 \Delta y_{t-2} + \ldots + \beta_p \Delta y_{t-p} + \varepsilon_t,$$ with drift coefficient c, deterministic trend coefficient δ, and AR(1) coefficient $\phi < 1$.

Figure 4.1: The Model Variants of the ADFtest [56]

To determine the stationarity state of the data, the sliding window method was used. The data for each subject contains 64 columns which is the number of the ROIs and between 200 to 390 rows which represents the time points. As the N-back task's duration was longer, the rows for it were more than the ones for the PVT session. The sliding window was applied for each ROI. There were some restrictions for selecting the size of the sliding window.

(1) The window size could not be more that 200 as in the fMRI dataset, the time points were at most 390, and we wanted to have a few sliding windows to go through the data. As a result, if the window size was too large, we would not be able to have multiple sliding windows.

(2) The PVT session had less time points compared to the N-back, and we wanted to apply the same settings for both of these tasks. For some subjects, there were only 200 time points or even less.

(3) For calculating the integration, a covariance matrix must be computed and for this aim, the number of time points (rows) must be equal or more than the number of columns. As a result, the minimum window size had to be more than the number of columns which is 64. We had to respect this restriction as we wanted to calculate the stationarity and the measure of integration in the same sliding windows.

Considering these three points, the stationarity analysis was performed for three different window sizes. Also, an overlap factor was included in the analysis. Alpha or the significance level was set to 0.05 and the model was tested for all three different versions of the ADF test considering the first and second orders of the AR model (lags).

The stationarity analysis was performed multiple times using the situations mentioned in table 4.1. As there were multiple properties that we could apply in our model, the effects of window size, models, lags, and overlap were individually investigated. At the end, we decided which properties were more important for us to include in the stationarity analysis.

Another important fact is that the stationarity analysis was first performed for each of the 64 ROIs. Afterwards, the average result over the ROIs for each session was calculated. We decided to show the average of the stationarity results for each session as the size of the results was too large (64 ROIs for each session, 13 sessions for each subject, 27 subjects in total).

		Window Sizes					
		70		100		150	
Models	AR	lag=1 ol=30%	lag=1 ol=40%	lag=1 ol=30%	lag=1 ol=40%	lag=1 ol=30%	lag=1 ol=40%
		lag=2 ol=30%	lag=2 ol=40%	lag=2 ol=30%	lag=2 ol=40%	lag=2 ol=30%	lag=2 ol=40%
	ARD	lag=1 ol=30%	lag=1 ol=40%	lag=1 ol=30%	lag=1 ol=40%	lag=1 ol=30%	lag=1 ol=40%
		lag=2 ol=30%	lag=2 ol=40%	lag=2 ol=30%	lag=2 ol=40%	lag=2 ol=30%	lag=2 ol=40%
	TS	lag=1 ol=30%	lag=1 ol=40%	lag=1 ol=30%	lag=1 ol=40%	lag=1 ol=30%	lag=1 ol=40%
		lag=2 ol=30%	lag=2 ol=40%	lag=2 ol=30%	lag=2 ol=40%	lag=2 ol=30%	lag=2 ol=40%

Table 4.1: Different Properties for Performing the Stationarity Analysis - Lag is the Order of the AR Model and Ol is the Overlap

4.1.1 The Effect of the Window Size

First, the stationarity analysis was performed for both N-back and PVT time-series which were parcelled with MIST-64 atlas. The following properties for the sliding window and adftest function were examined.

In the first test, the window sizes 70, 100 and 150, the overlap of 30% and 40%, the first and second lagged versions of the AR model, and the AR, ARD and TS models were tested. The results for N-back and PVT sessions are shown in Figures 4.2 - 4.7. For each model, twelve different cases were examined. The x-axis in each figure represents the fMRI sessions and for the y-axis, as the number of time points (rows) in different sessions were different, a desirable number (500) was chosen, and the total time points for the dataset related to different sessions of each subject were scaled to 500. In the figures, the sliding windows which go through the whole data are shown in different colors (dark blue for the first sliding window, red for the second sliding window, lime color for the third sliding window, and so on). The color "gray" represents the percentage of non-stationarity in each sliding window. In the PVT session, as the number of rows were much less than the N-back task, the last sliding window did not contain enough time points. For example, in Figure 4.5, when the window size was 100 and the overlap is 30%, the window size got larger than the total number of time points, which is why you see a greater gray part in its results. This does not show

the percentage of non-stationarity. It just means that not enough time points were available.

Figure 4.2: Calculating Stationarity in AR Model for 12 Different Cases - N-Back Session

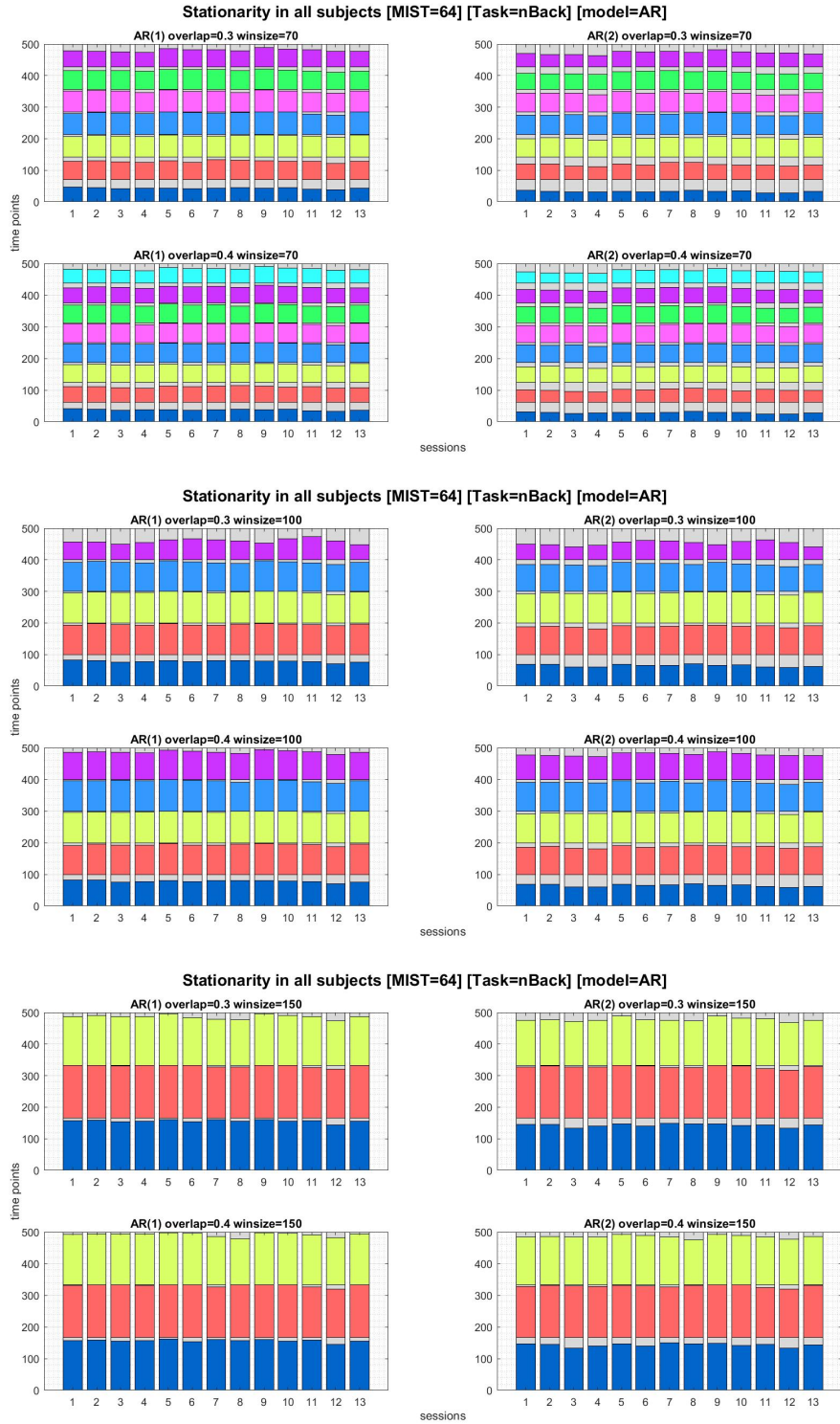Figure 4.3: Calculating Stationarity in ARD Model for 12 Different Cases - N-Back Session

Figure 4.4: Calculating Stationarity in TS Model for 12 Different Cases - N-Back Session

Figure 4.5: Calculating Stationarity in AR Model for 12 Different Cases - PVT Session
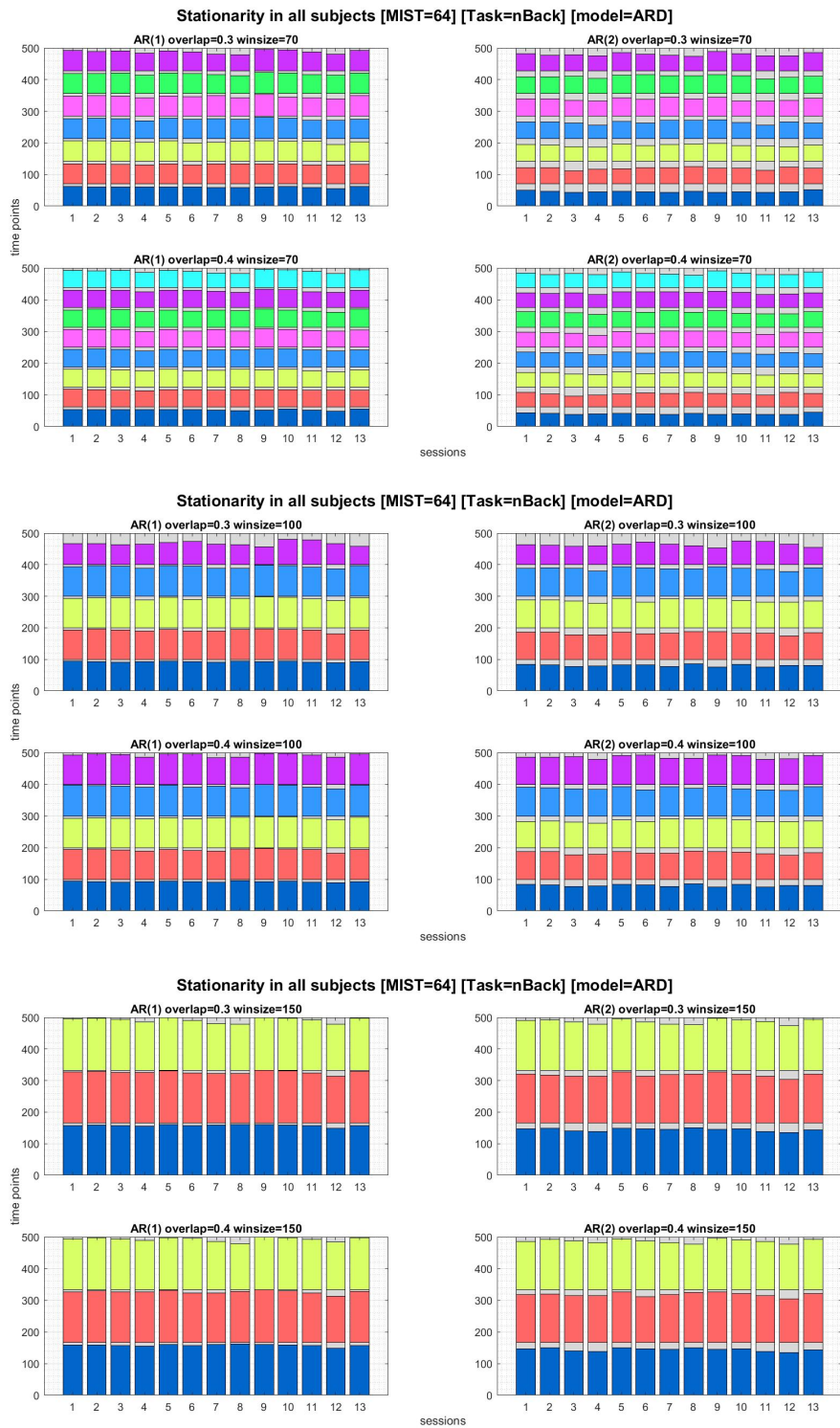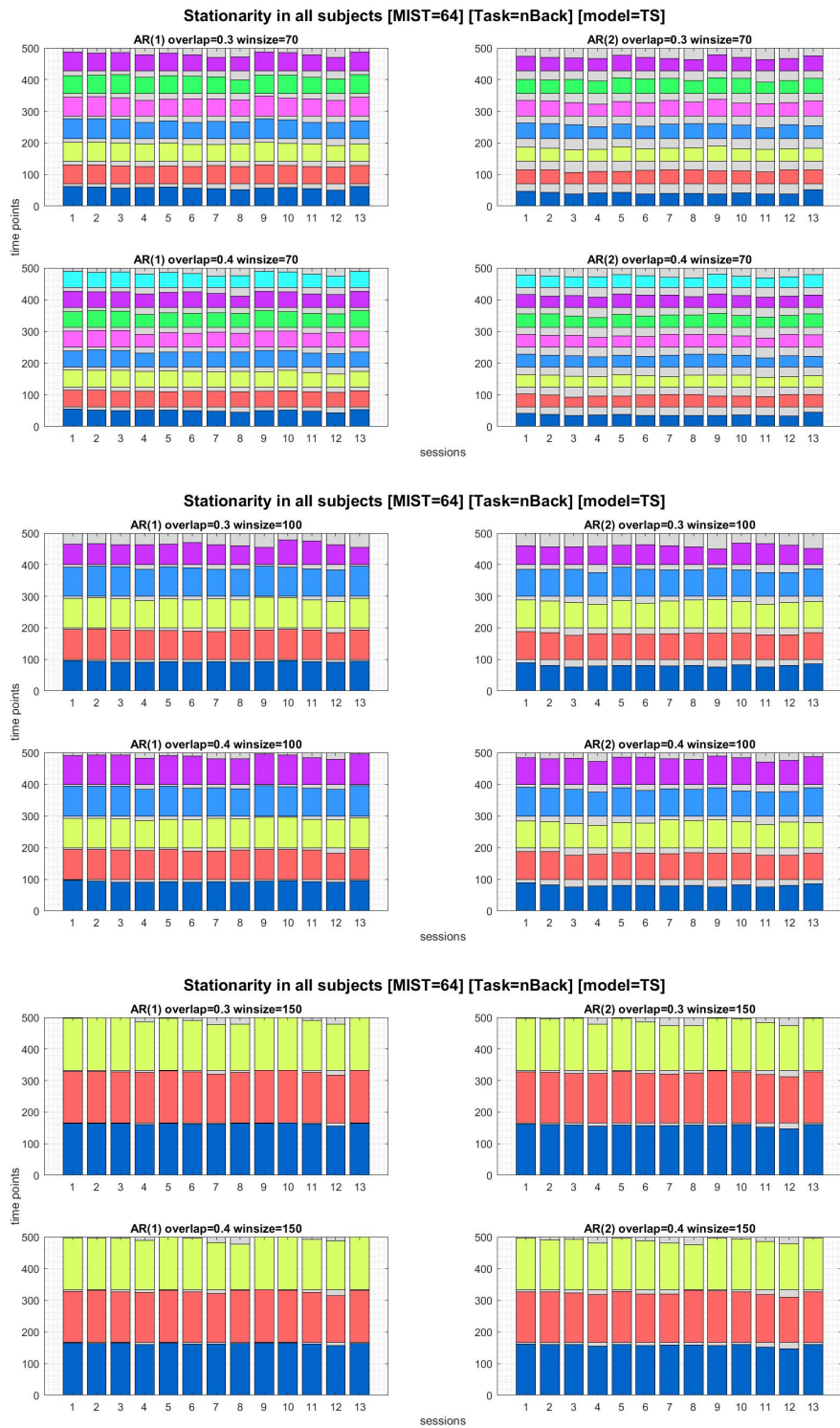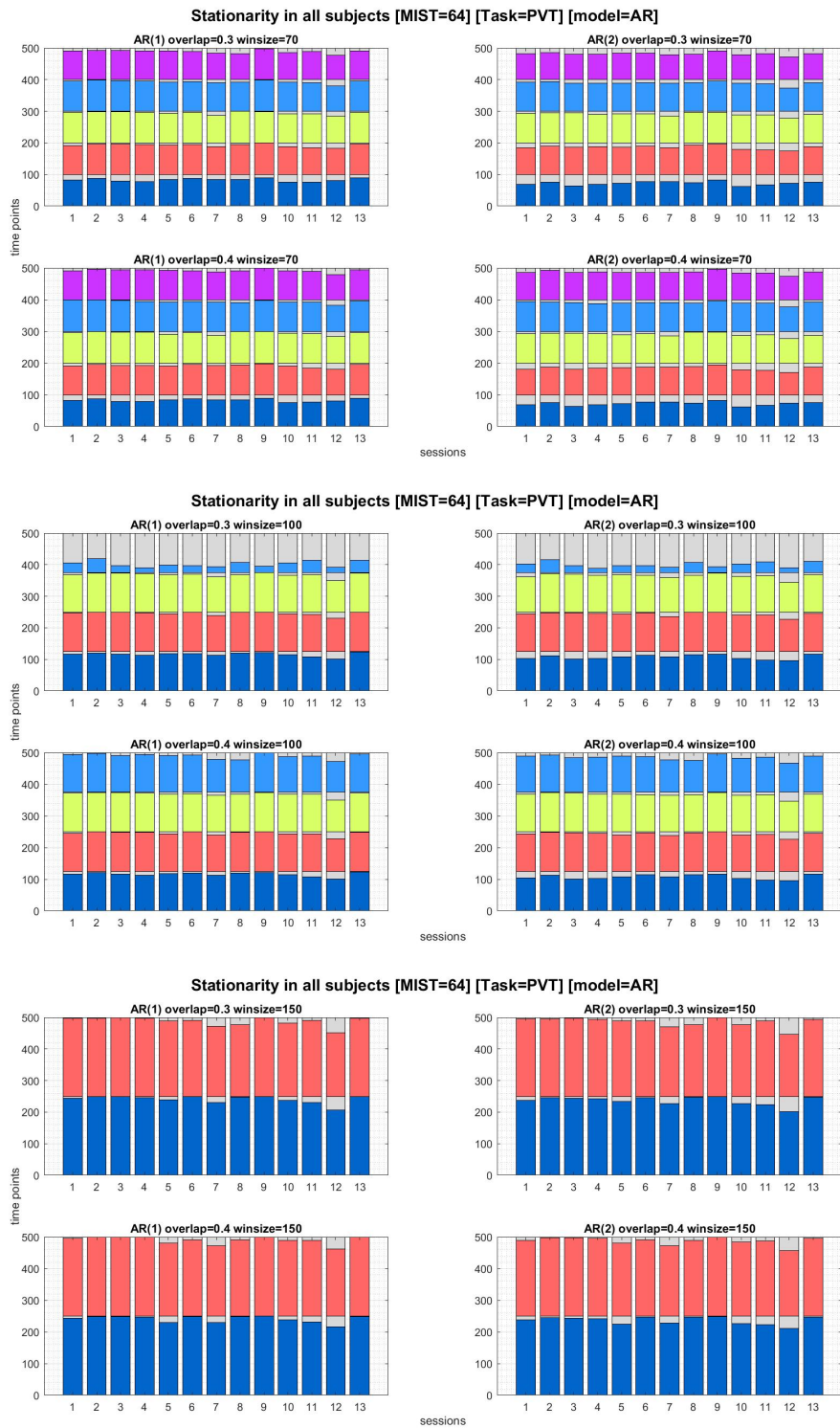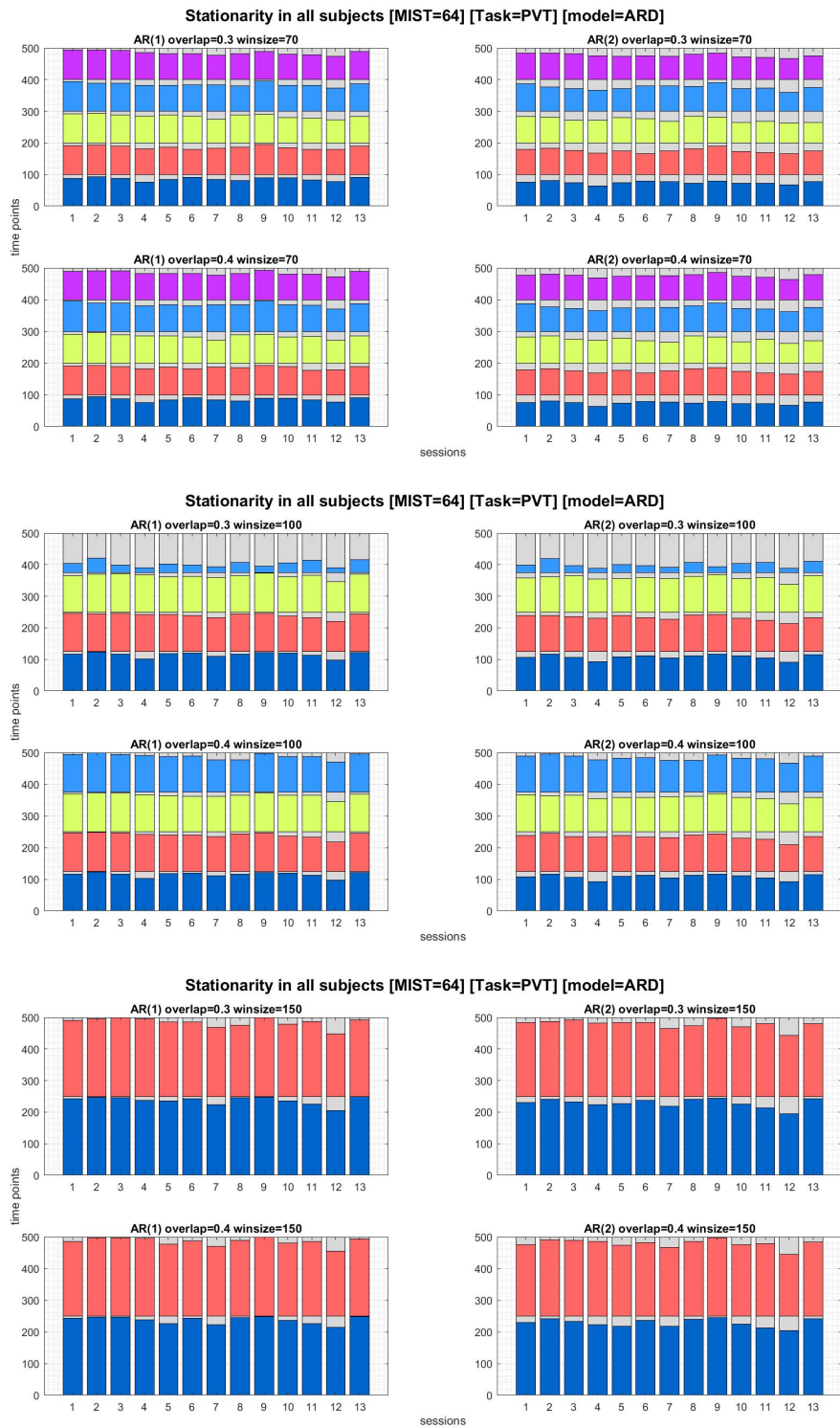
Figure 4.6: Calculating Stationarity in ARD Model for 12 Different Cases - PVT Session
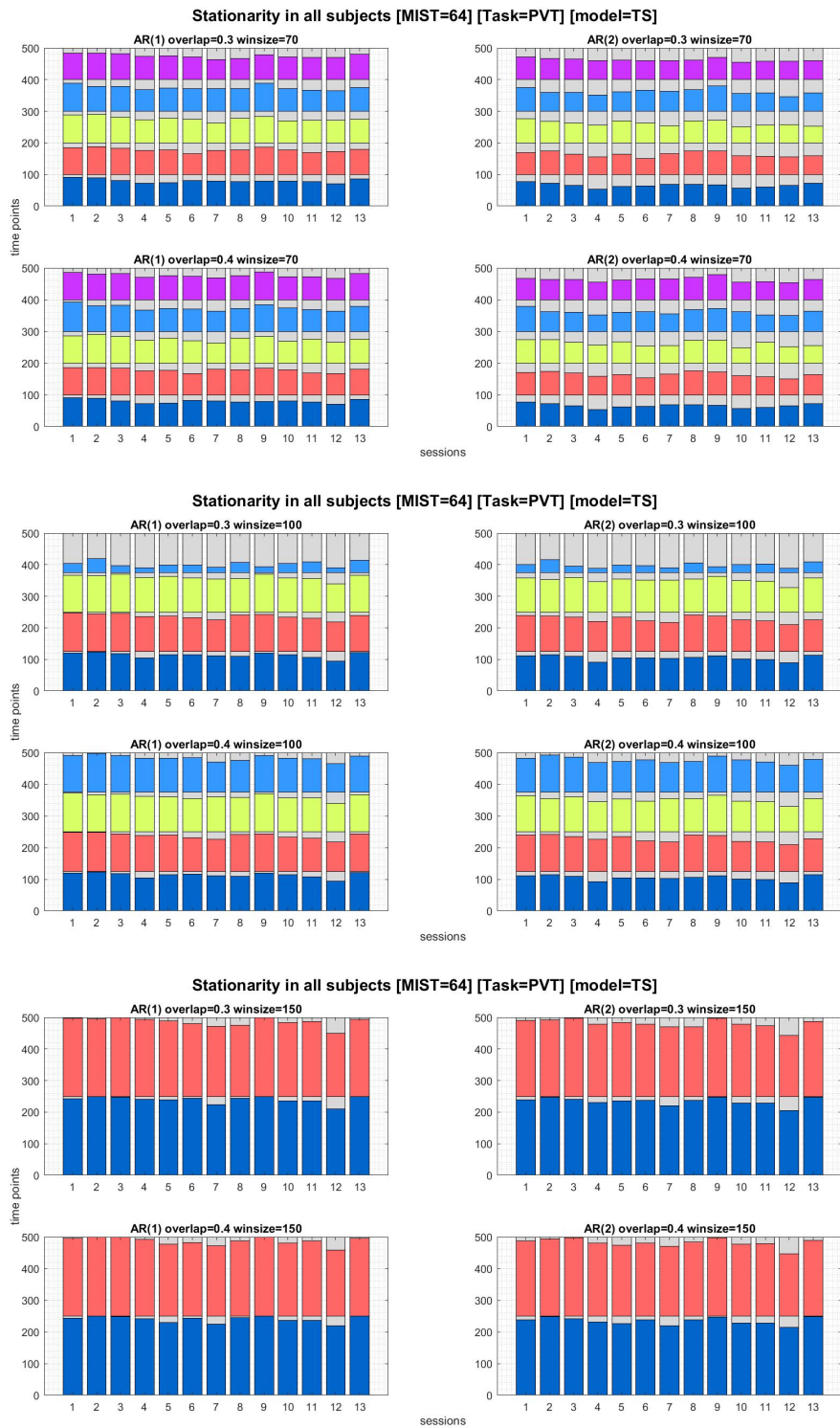
Figure 4.7: Calculating Stationarity in TS Model for 12 Different Cases - PVT Session

Looking at this data, the first thing we can conclude is that by enlarging the size of the sliding window, more stationarity is detected in the time-series. A very small sliding window might be too strict in detecting stationary parts of the data and it will be very sensitive to noise and fluctuations. On the contrary, a very large sliding window might miss some important information and be less sensitive to vital changes in the time-series. So, at this point we decided to choose the size of 100 for the sliding window and repeat the analysis to make a decision about the rest of the properties.

4.1.2 The Effect of the Lags

Considering our results in the first test, for the second test, the window size 100 was used. Also, in this test we did not use any overlap, but the rest of the properties for this test was the same as the previous one; the lags of 1 and 2, and the AR, ARD and TS models were tested. The results of this analysis are shown in Figures 4.8 and 4.9. The first thing this result shows is that by using window size of 100 with no overlap, only three sliding windows are needed to go through the whole data. Also, using less parameters, we can now see the effects of using different models of AR, ARD and TS, and having different lags of 1 and 2 for the ADF test. As the results of different models seem to be very close, at this level we chose to continue the analysis using all three models. Regarding the lags of the AR model, lag 2 was chosen as we believe that the past values of the fMRI time-series influence the current value and it is better to consider two lagged versions of the data in the analysis.

4.1.3 The Effect of the Overlaps

In the third test, the analysis was done for the window size of 100, lag of 2, overlap of 30% and 40%, and AR, ARD and TS models. As shown in Figures 4.10 and 4.11, using overlaps of 30% and 40%, five sliding windows for the N-back and four windows for the PVT were needed to slide through the whole data and for all three models, the results seem to be very close although at some parts when overlap is 40%, more stationarity was detected in the time-series. But still, comparing the results of Figures 4.8 and 4.10, or Figures 4.9 and 4.11, it can be seen that having no overlaps or 30% - 40% overlaps in the analysis do not have a considerable effect in detecting stationarity in the time-series. As a result of this, in the succeeding analysis, we did not use any overlaps.

Figure 4.8: Calculating Stationarity for Different Lags - N-Back Session

Figure 4.9: Calculating Stationarity for Different Lags - PVT Session

Figure 4.10: Calculating Stationarity for Different Overlaps - N-Back Session

Figure 4.11: Calculating Stationarity for Different Overlaps - PVT Session

4.1.4 The Effect of different Models

In the last test, the effects of using different models of AR, ARD and TS were assessed. As shown in Figures 4.12 and 4.13, the results for the different models almost look the same. However, it seems that the AR and the ARD models' results in the different sliding windows are much better than the TS model. Moreover, in all three models more stationarity was detected in the second and third sliding windows compared to the first sliding window. This might be the result of the habituation effect in the individuals at the first moments that they were in the MR scanner.
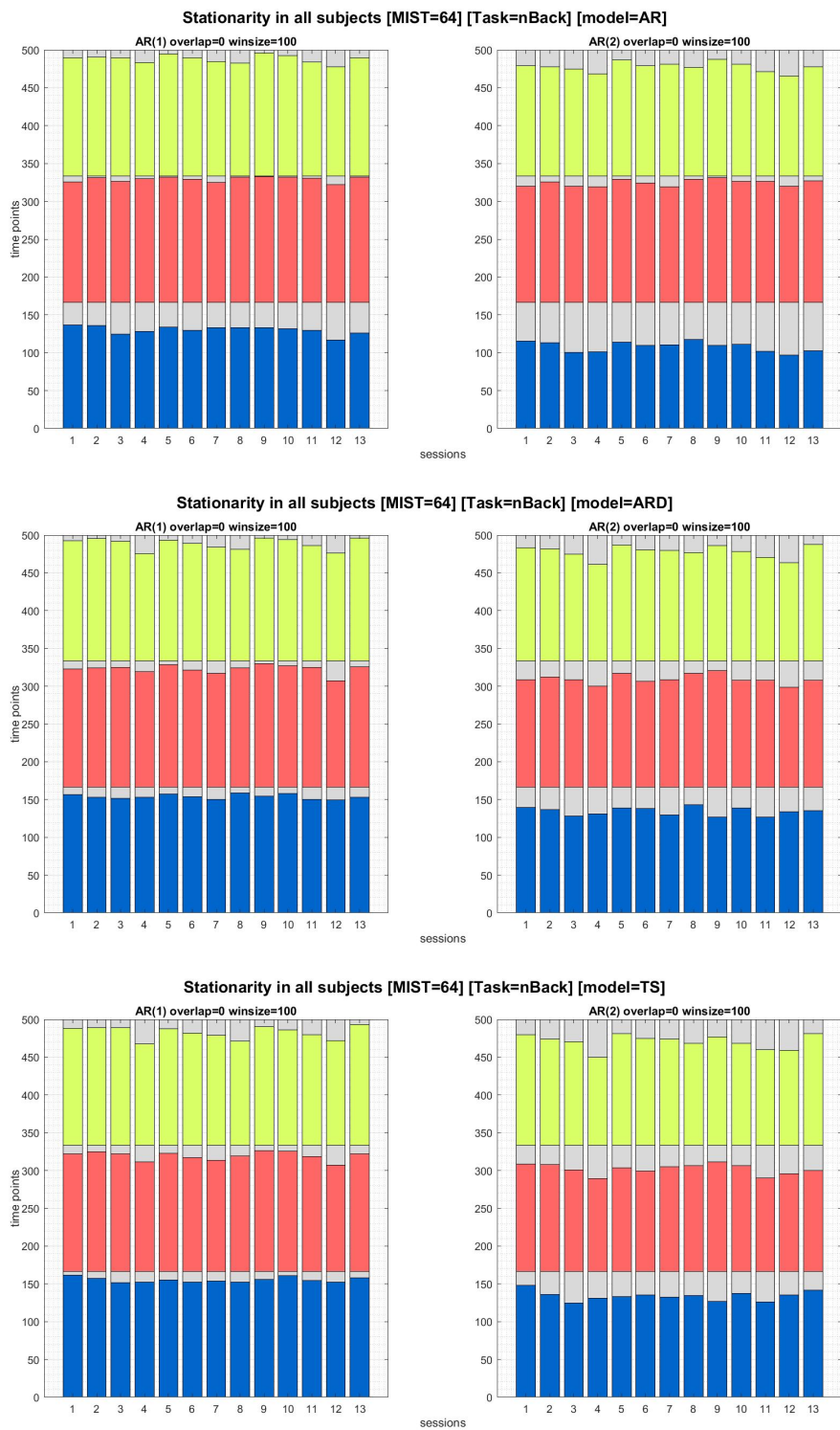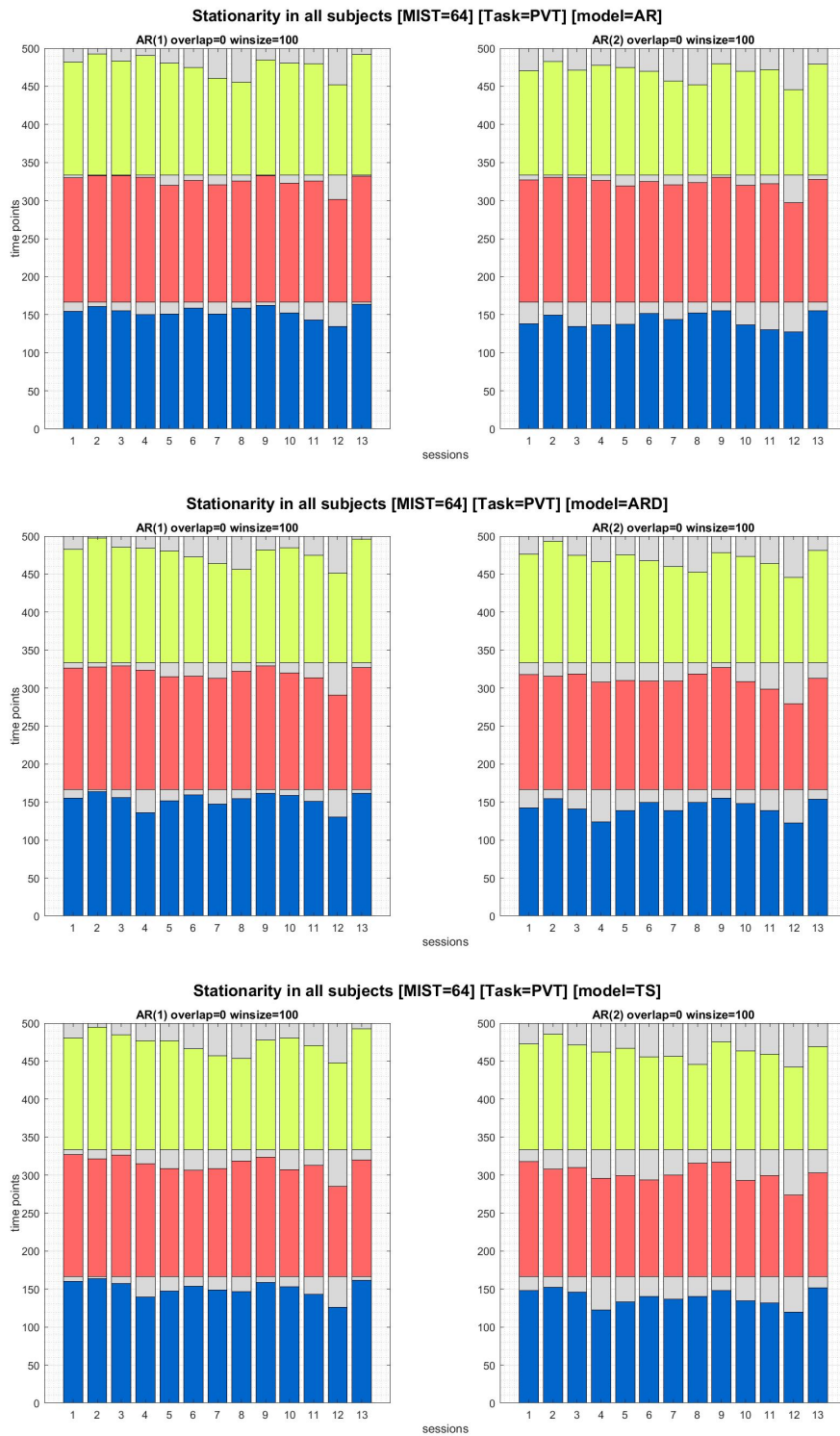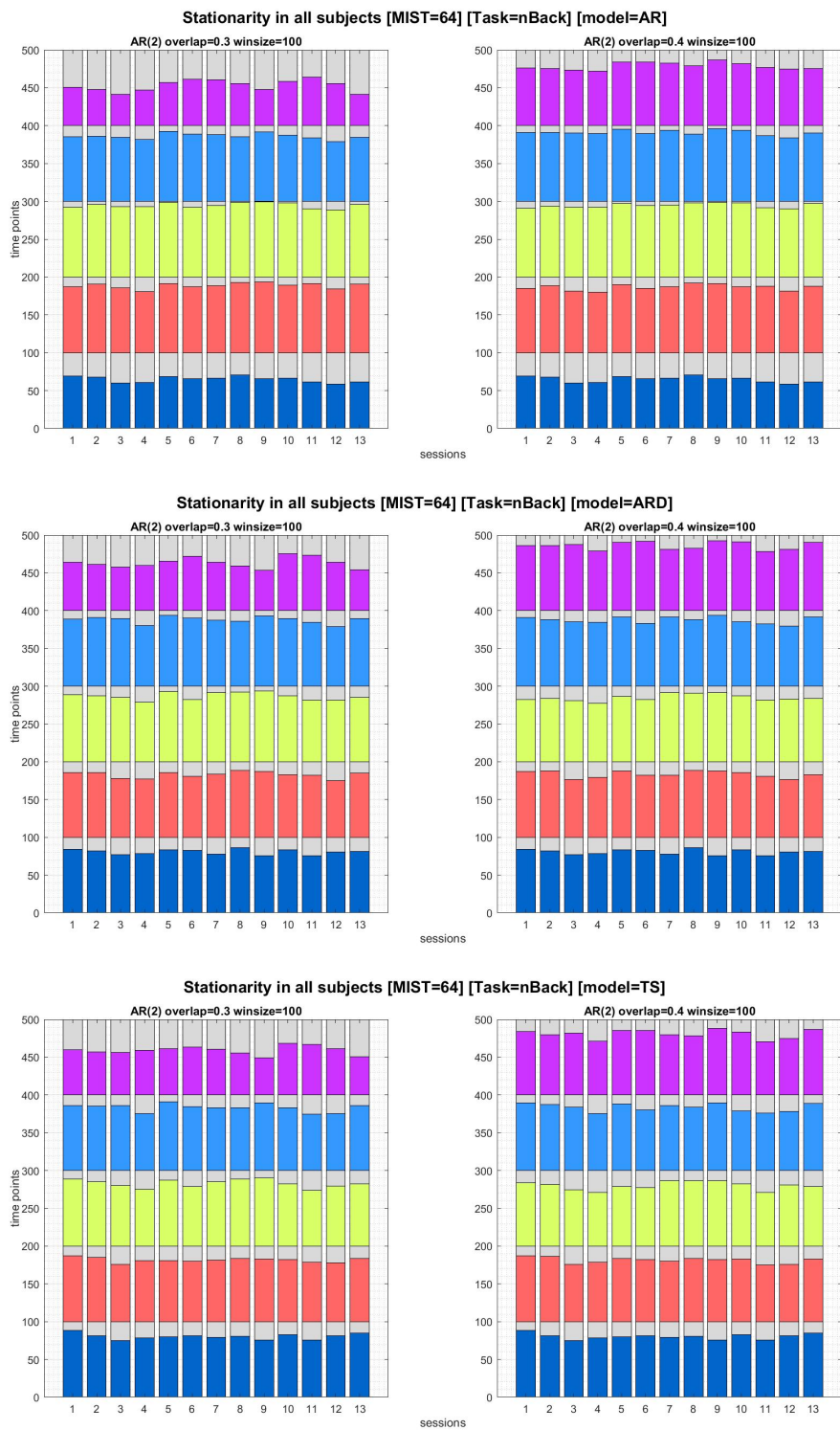

Figure 4.12: Calculating Stationarity for Different Models - N-Back Session

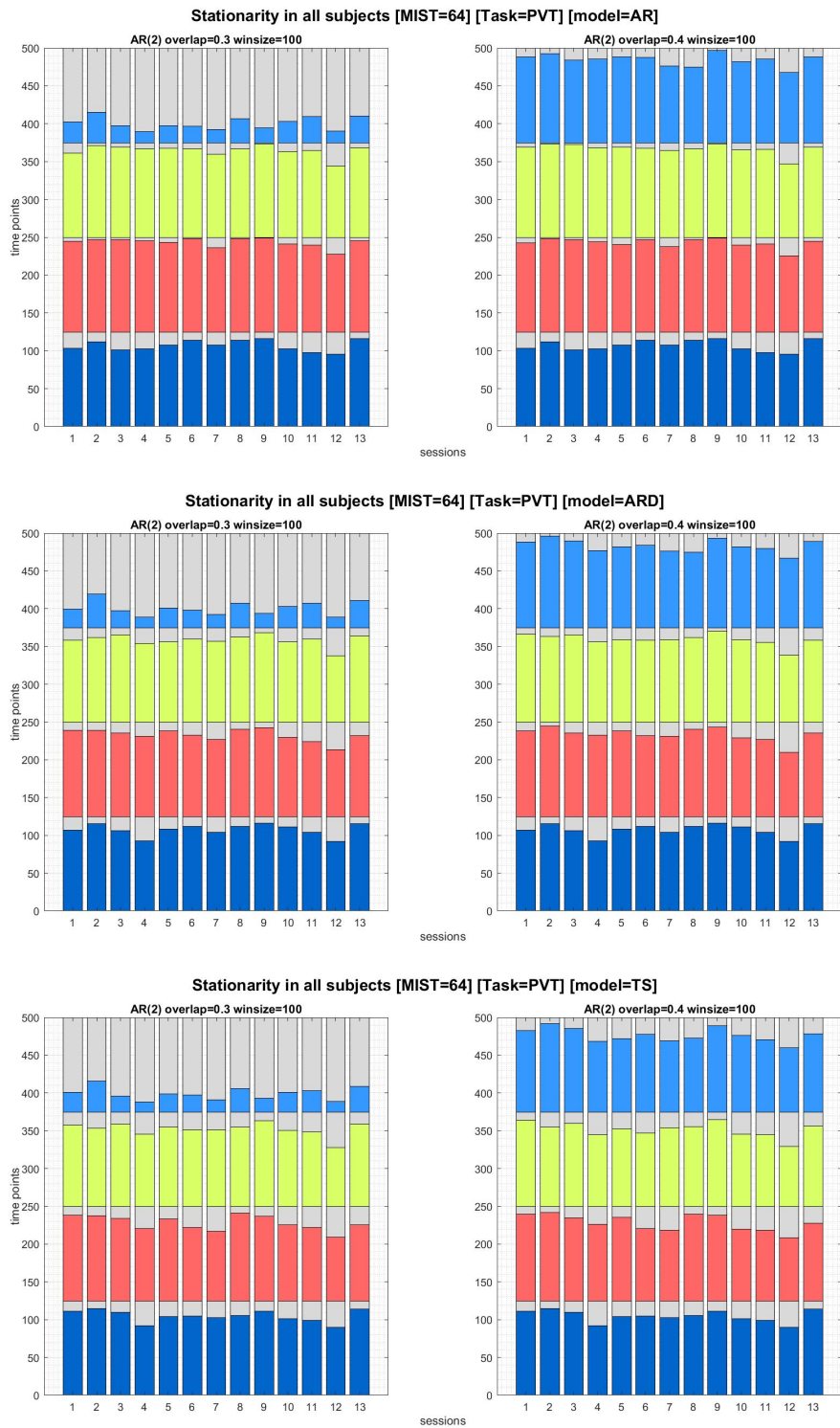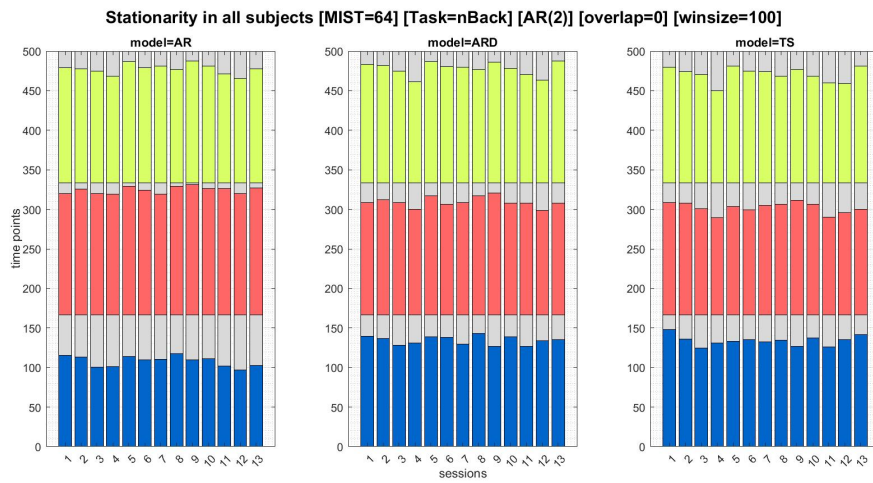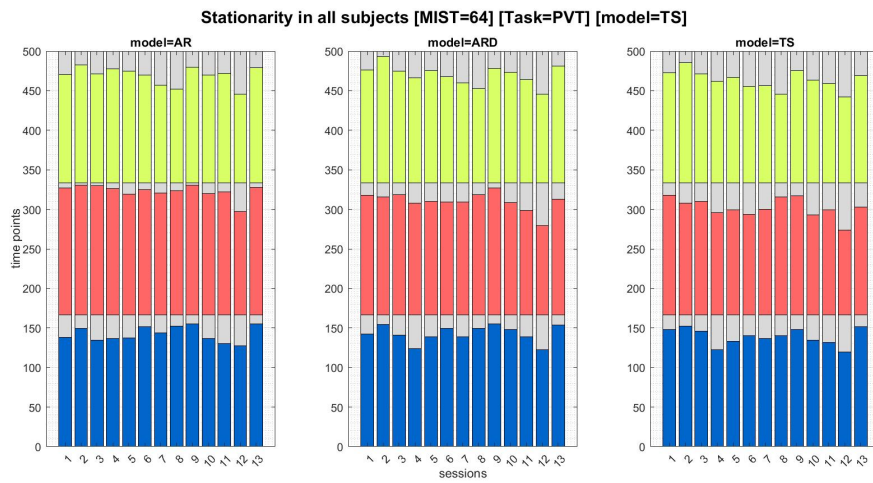Figure 4.13: Calculating Stationarity for Different Models - PVT Session

A goal of this research is to calculate the measure of integration for a stationary and non-stationary sliding window. As a result, we decided to do the stationary analysis with the AR model, and compute the integration for the first and second sliding windows to see how the results of the integration change in stationary and non-stationary sliding windows.

4.2 Hierarchical Integration for the FMRI Time-series

In this section the Hierarchical Integration (HI) was calculated for each subject using the sliding window method. As in section 4.1 we decided to use the sliding window of size 100 with no overlaps, we will continue the experiment using the same setting. Moreover, as explained in the previous section, the chosen properties for calculating the stationarity using the adftest are a lag of 2 and the AR model.

Figures 4.14 and 4.15 show the results of total integration in three different subjects for N-back and PVT sessions, respectively. In each figure of each subject, two plots are shown which contain the results of stationarity of the data within the sliding window (the red area), total integration (the yellow curve), the melatonin (the blue curve) and the sleep pressure (or sleep drive, the pink line). In the first sliding window for all the subjects the data is less stationary than the second sliding window, and this result is shown as a red area. In all the figures, the x-axis is related to the time for which each session was performed and the y-axis has an amplitude of one as all the results are normalized to be between zero and one, so that they would become comparable.

Looking at the results, it can be seen that when the data is not stationary, the results of the measure of integration contain a lot of fluctuations. Meanwhile, for the stationary time windows, it seems that in general, the measure of integration follows the melatonin's curve. However, in the non-stationary time windows, this pattern is not evident.

The second result is that all the subjects had two peaks in their melatonin data which happened at a time between 23:00 to 5:00 of the second day and after 1:00 of the third day. Also, in most of the subjects, the total integration had two peaks and these peaks happened around the same time as the melatonin's curve. However, the peak of melatonin and the total integration were not completely aligned with each other.
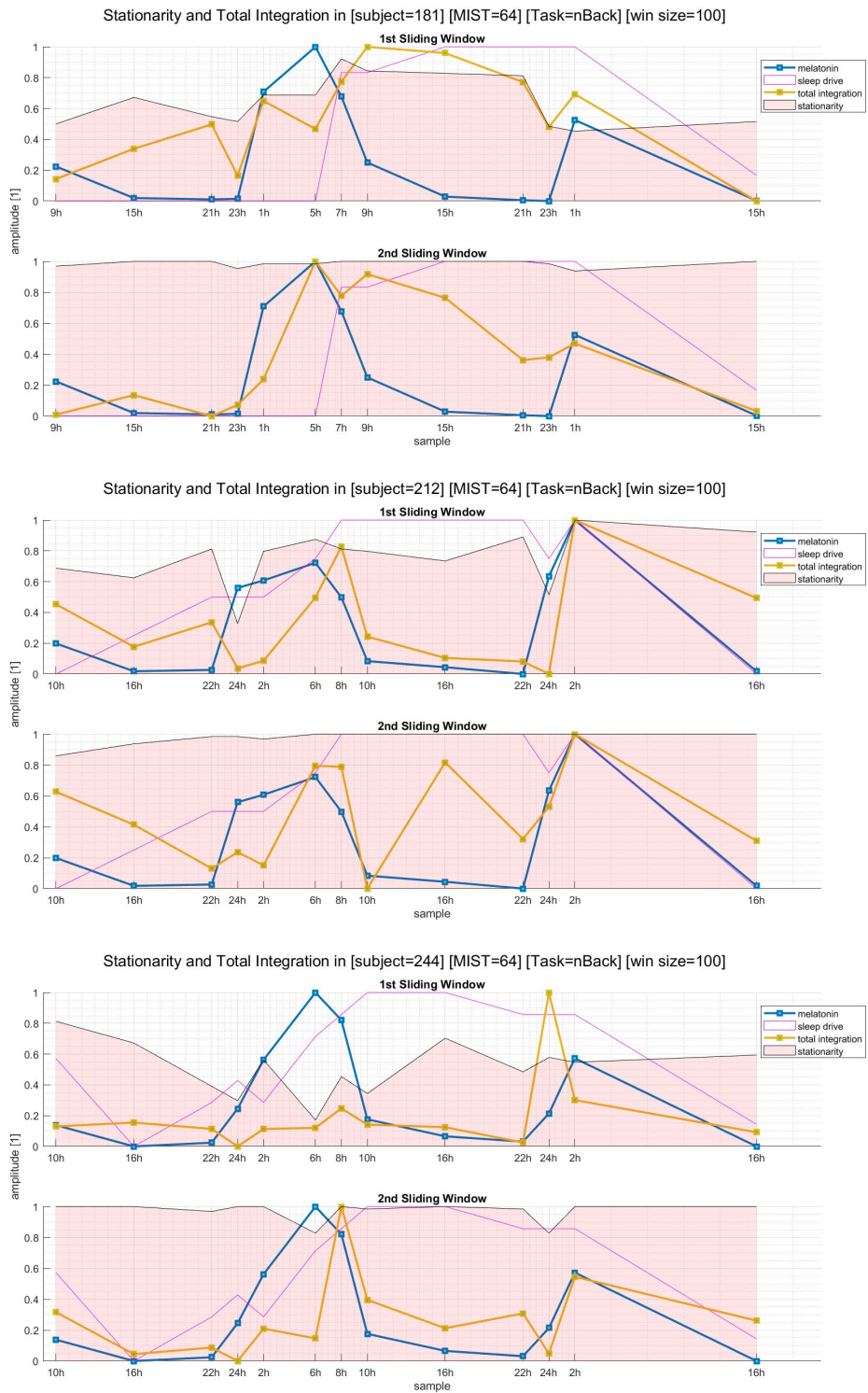
Figure 4.14: Results of Total Integration for Stationary and non-Stationary Time Windows in the Time-series of the N-back Session for Three Different Subjects
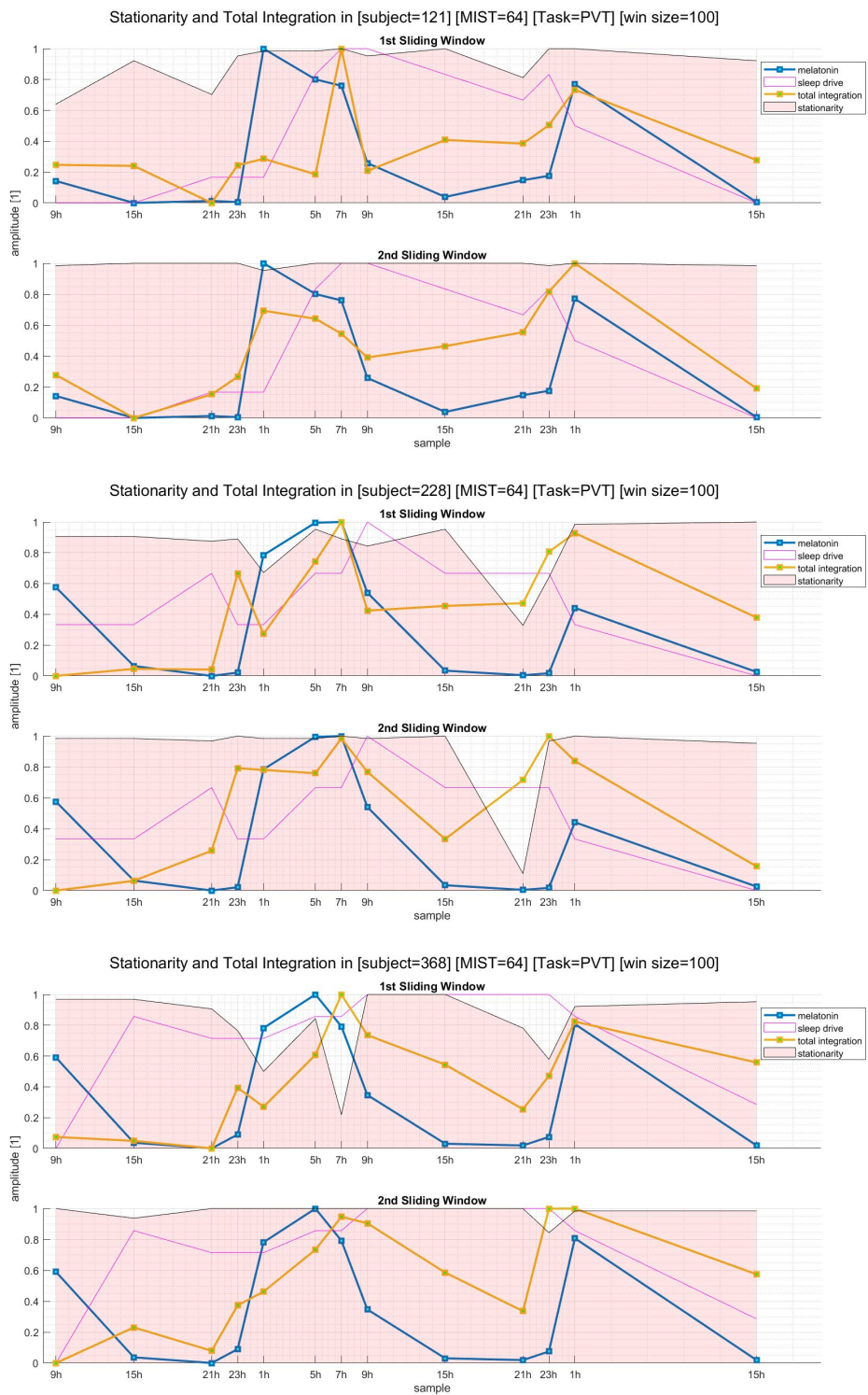
Figure 4.15: Results of Total Integration for Stationary and non-Stationary Time Windows in the Time-series of the PVT Session for Three Different Subjects

Third, as shown in the results, although it seems that total integration is following the melatonin's curve, there are some parts where these measures are not completely aligned and their slops are dissimilar. This fact suggests that there might be another factor which has an effect on the measure of integration which is not considered in this research. Moreover, this irregular pattern which can be seen for some of the subjects might be the result of the individual differences.

Figure 4.16: Results of Total Integration for Stationary Sliding Window in the Time-series of N-back and PVT Sessions of All Subjects

Another analysis performed on the measure of integration was comparing the results of the first and second days of the subjects. Our aim was to see how integration changes in SD condition. For this aim, the total integration dataset was divided into two sets: Wakefulness (Day1) and Sleep Deprivation (Day2), and a comparison between these two sets was done which is shown in Figure

4.16. The wakefulness part (shown in blue) is the data of the first day of the experiment in the laboratory from morning to midnight, and the sleep deprivation part (shown in orange) is related to the second day of the experiment after getting no sleep during the night. The x-axis shows the times of the data acquisition and the y-axis shows the amplitude of the measure of integration.

I_{tot}	Wakefulness		Sleep Deprivation	
Time	Mean	Std	Mean	Std
9h	87.286	1.948	101.956	2.150
15h	84.342	1.919	93.414	2.066
21h	85.453	1.912	88.406	1.985
23h	87.958	1.946	94.879	2.058
1h	92.521	1.986	103.216	2.126

(a) N-back Session

I_{tot}	Wakefulness		Sleep Deprivation	
Time	Mean	Std	Mean	Std
9h	90.128	2.021	110.635	2.237
15h	88.657	1.985	105.814	2.165
21h	90.068	2.036	99.649	2.136
23h	94.317	2.060	113.463	2.632
1h	103.222	2.142	112.037	2.274

(b) PVT Session

Table 4.2: Total Integration Results For Wakefulness and Sleep Deprivation Conditions

The summary of the results for total integration is recorded in Table 4.2 which shows that I_{tot} in SD increased compared to the wakefulness condition as there was a growth in both I_{ws} and I_{bs} in the second day. Although an increase was noticed in both I_{ws} and I_{bs} on the second day, the change in between-system integration was proportionally greater than the within-system integration.

4.3   FCR for the FMRI Time-series

For calculating the FCR, like the previous section, the data was divided into two sets: Wakefulness and Sleep Deprivation, and a comparison between these two sets was done which is shown in Figure 4.17. The x-axis shows the times of the data acquisition and the y-axis shows the amplitude of the FCR.

Looking at the results in Table 4.3 and Figure 4.17, it is evident that the FCR is reduced in

sleep deprivation condition compared to the wakefulness in both N-Back and PVT sessions. At the subject level also for most of the individuals a decrease in FCR during the SD situation compared to the wakefulness was found.
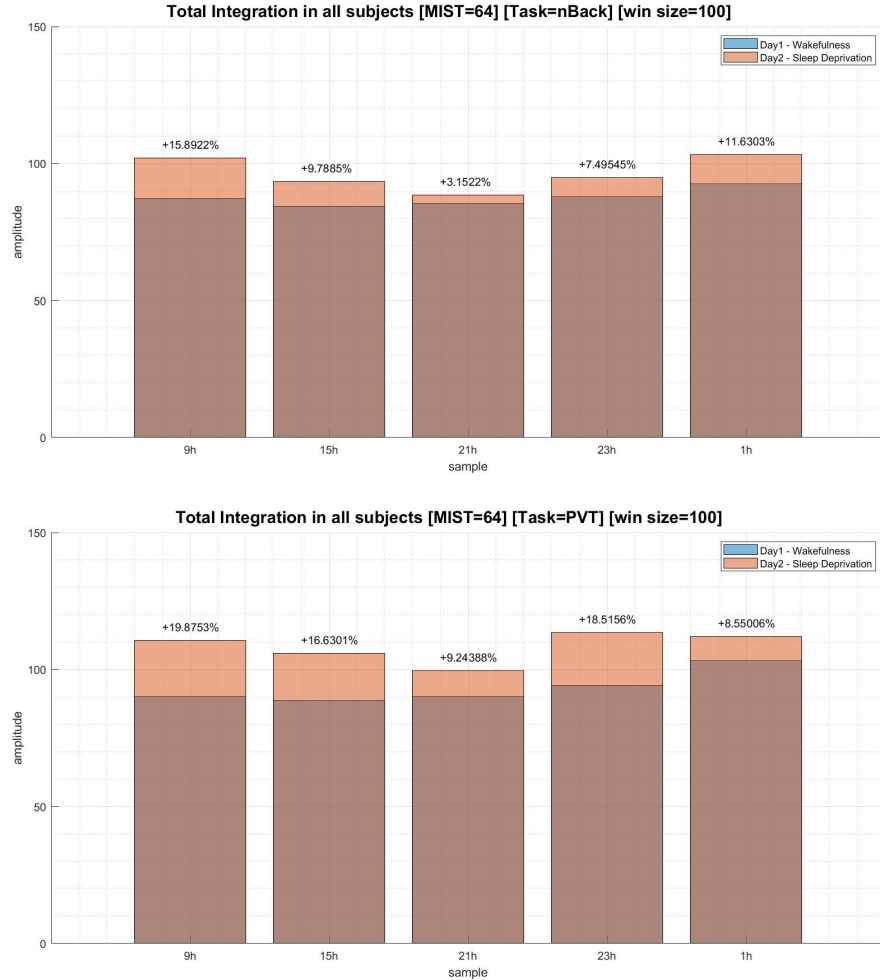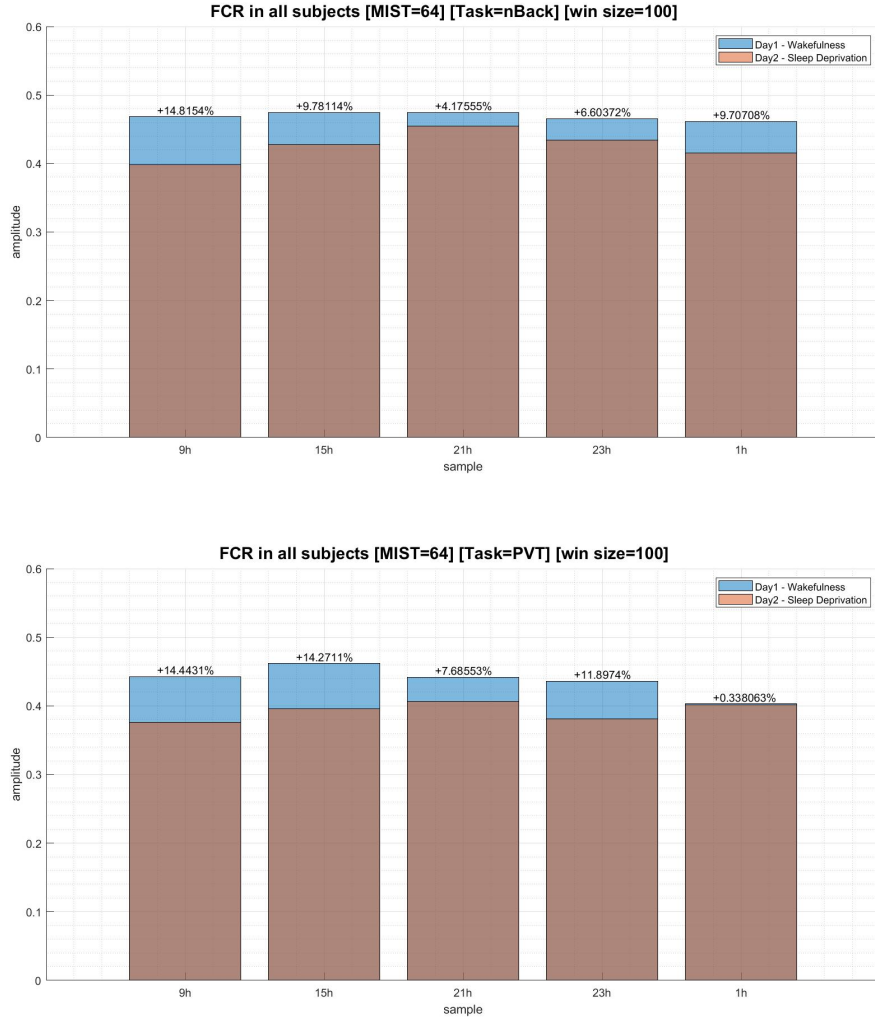

Figure 4.17: Results of FCR for Stationary Sliding Window in the Time-series of N-back and PVT Sessions of All Subjects

As mentioned in section 4.2, there was an increase in both I_{ws} and I_{bs}, but the increase in I_{bs} was much larger that the increase in I_{ws}. As a result of this, we had a decrease in FCR values. Moreover, as FCR is a ratio of functional segregation, this suggests that the brain's modularity decreases in SD condition while the functional integration increases.

$FCR = I_{ws}/I_{bs}$	Wakefulness		Sleep Deprivation	
Time	Mean	Std	Mean	Std
9h	0.468	0.034	0.398	0.029
15h	0.474	0.035	0.428	0.033
21h	0.475	0.034	0.455	0.034
23h	0.465	0.033	0.434	0.032
1h	0.462	0.033	0.415	0.030

(a) N-back Session

$FCR = I_{ws}/I_{bs}$	Wakefulness		Sleep Deprivation	
Time	Mean	Std	Mean	Std
9h	0.443	0.034	0.376	0.027
15h	0.462	0.034	0.396	0.028
21h	0.442	0.034	0.406	0.029
23h	0.436	0.033	0.381	0.030
1h	0.403	0.029	0.401	0.029

(b) PVT Session

Table 4.3: FCR Results For Wakefulness and Sleep Deprivation Conditions

4.4 The GLM Results

In this part, the relationship between the Melatonin, Total Integration, the Sleep Pressure and the FCR is examined. For this aim, a GLM was designed to see whether the values of the total integration, sleep pressure and FCR have any linear relationship with the melatonin values or not. The equation that was examined through GLM is as follows.

$$Melatonin \sim 1 + HI + KSS + FCR \qquad (36)$$

In this equation, KSS represents the sleep pressure. To check if there is any linear relationship, the GLM was tested for each subject and the results are shown in Figure 4.18. In this figure, the x-axis represents the subjects and the y-axis is the amount of the p-value. The yellow bar is the p-velue for the sleep pressure, the purple bar is the p-value for the total integration, and the blue line represents the p-values for the FCR. The red dashed-line shows the place where the p-value is 0.05, and if any amount falls bellow this line, it means it is significant. The figures display that the p-value of the coefficients of sleep pressure are much higher than the significance level which is 0.05. This suggests that there is no linear relationship between KSS and melatonin which is a predetermined

result. From the definitions of melatonin and sleep pressure (Section 1.2), we know that these two parameters regulate separately and without any dependence on one another.
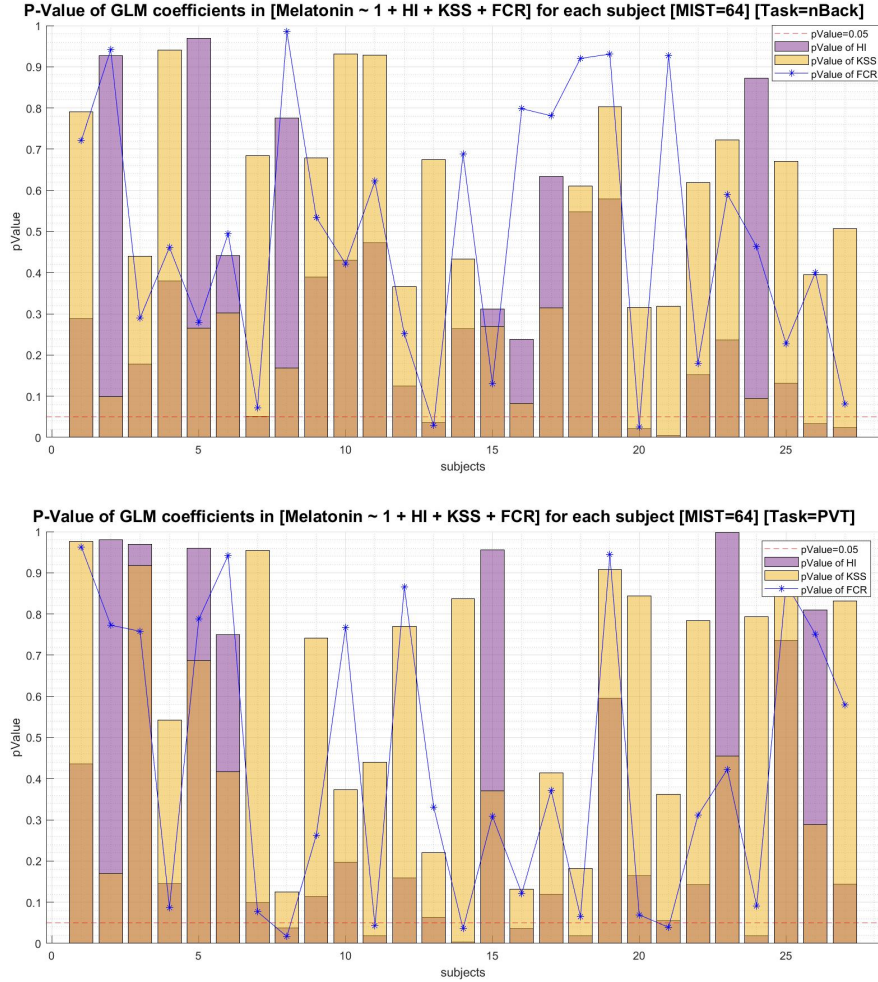
Figure 4.18: P-Value of GLM Coefficients in All Subjects - N-back and PVT Sessions

Moreover, the p-values of the coefficients of the total integration and FCR, are also higher than 0.05, but in some cases this value is close to 0.05, and for some subjects, it is less than 0.05. As a result, we can conclude that in general the total integration and FCR do not have a linear relationship with the melatonin but in some of the subjects, a dependency between total integration and melatonin, and FCR and melatonin can be detected.

4.5 The ANOVA Test Results

The ANOVA test was performed on the FCR and the total integration results of all subjects to make different comparisons.

The first test case was to observe how total integration and FCR change in wakefulness and sleep deprivation situations. Table 4.4 shows the results of the ANOVA test on FCR results in N-back and PVT sessions. In this table, "Columns" represent all 27 subjects, and "Rows" represent the FCR values of the first and the second days each of which includes five fMRI sessions. The column $Prob > F$ shows the p-values for the analysis on the subjects (0 for N-back and PVT), the wakefulness and SD conditions (0 for N-back and PVT), and the interaction between the subjects and the two conditions (0.0012 for N-back and 0.031 for PVT). All the p-values are significant in the table. Here is a summary of the conclusion that can be made from this result:

(1) The subjects' means for FCR are significantly different from each other, meaning that each subject's FCR is different from the other subjects.

(2) The two conditions (wakefulness and SD) means are significantly different from each other, meaning that the FCR values for wakefulness and SD are different from each other.

(3) There is an interaction between the subjects' and the conditions' FCR means.

Table 4.5 shows the results of the ANOVA test between Day1 (Wakefulness) and Day2 (Sleep Deprivation) at the group level on the FCR results for N-back and PVT sessions. In this table, "Group A" refers to Day1, and "Group B" refers to Day2. The p-values for both N-back and PVT sessions are significant (6.325e-09 and 7.350e-15, respectively) which suggests that the FCR's mean value between wakefulness and SD conditions are significantly different. Moreover, as the value for column A-B is positive, it means that the mean value of FCR for the wakefulness situation is more than the mean value of FCR for the SD situation. This result supports our conclusion in section 4.3.

Table 4.6 shows the results of the ANOVA test on the total integration between wakefulness and SD conditions in N-back and PVT sessions. Similar to Table 4.4, the p-values for the 27 subjects, the wakefulness and SD conditions, and the interaction between the subjects and the two conditions are significant which suggest that:

Source	SS	df	MS	F	Prob>F
Columns	0.353	26	0.01358	3.54	0
Rows	0.12362	1	0.12362	33.2	0
Interaction	0.21943	26	0.00844	2.2	0.0012
Error	0.82917	216	0.00384		
Total	1.52521	269			

(a) N-back Session

Source	SS	df	MS	F	Prob>F
Columns	0.2614	26	0.01005	2.54	0.0001
Rows	0.13622	1	0.13622	34.4	0
Interaction	0.16759	26	0.00645	1.63	0.0329
Error	0.85527	216	0.00396		
Total	1.42048	269			

(b) PVT Session

Table 4.4: ANOVA Results for FCR Between Wakefulness and Sleep Deprivation Conditions

Group A	Group B	Lower Limit	A - B	Upper Limit	P-value
1	2	0.028	0.043	0.058	1.388e-08

(a) N-back Session

Group A	Group B	Lower Limit	A - B	Upper Limit	P-value
1	2	0.029	0.045	0.059	4.473e-9

(b) PVT Session

Table 4.5: ANOVA Results for FCR - Comparison Between Day1 and Day2

(1) The subjects' total integration means are significantly different from each other.

(2) The two conditions' (wakefulness and SD) total integration means are significantly different from each other.

(3) There is an interaction between the subjects' and the conditions' total integration means.

Table 4.7 shows the results of the ANOVA test between Day1 (Wakefulness) and Day2 (Sleep Deprivation) at the group level on the total integration results for N-back and PVT sessions. As the p-values for both N-back and PVT sessions are significant (6.989e-11 and 7.317e-15, respectively), we can conclude that the total integration mean values between wakefulness and SD conditions are significantly different. Besides, the value for column A-B is negative which means that the mean value of the total integration for the wakefulness situation is less than the mean value of the

Source	SS	df	MS	F	Prob>F
Columns	16564.4	26	637.09	4.29	0
Rows	6311.2	1	6311.25	42.51	0
Interaction	9269.8	26	356.53	2.4	0.0003
Error	32071.3	216	148.48		
Total	64216.8	269			

(a) N-back Session

Source	SS	df	MS	F	Prob>F
Columns	19166.8	26	737.2	2.9	0
Rows	15294.4	1	15294.4	60.27	0
Interaction	10897.1	26	419.1	1.65	0.029
Error	54814.5	216	253.8		
Total	100172.8	269			

(b) PVT Session

Table 4.6: ANOVA Results for Total Integration Between Wakefulness and Sleep Deprivation Conditions

total integration for the SD situation which suggest that the functional integration increases in SD condition.

Group A	Group B	Lower Limit	A - B	Upper Limit	P-value
1	2	-12.576	-9.669	-6.763	6.989e-11

(a) N-back Session

Group A	Group B	Lower Limit	A - B	Upper Limit	P-value
1	2	-18.853	-15.053	-11.252	7.317e-15

(b) PVT Session

Table 4.7: ANOVA Results for Total Integration - Comparison Between Day1 and Day2

In the second test case, a comparison was made between the results of the total integration and FCR for the two last fMRI sessions (12th and 13th). As mentioned in chapter 3, after the 12th session, all the subjects had a 12-hour recovery sleep followed by the 13th fMRI session which was performed an hour after the participants woke up.

Figure 4.19, shows the results of a comparison between the total integration of the two last sessions. The total integration values for the 12th and 13th sessions are shown in pink and blue, respectively. As displayed in the figure, the mean values of the total integration for the two final sessions were different from each other, and an interesting result is that the total integration's mean

value of the 13th session (wakefulness condition) is less than the mean value of the 12th session (SD condition).
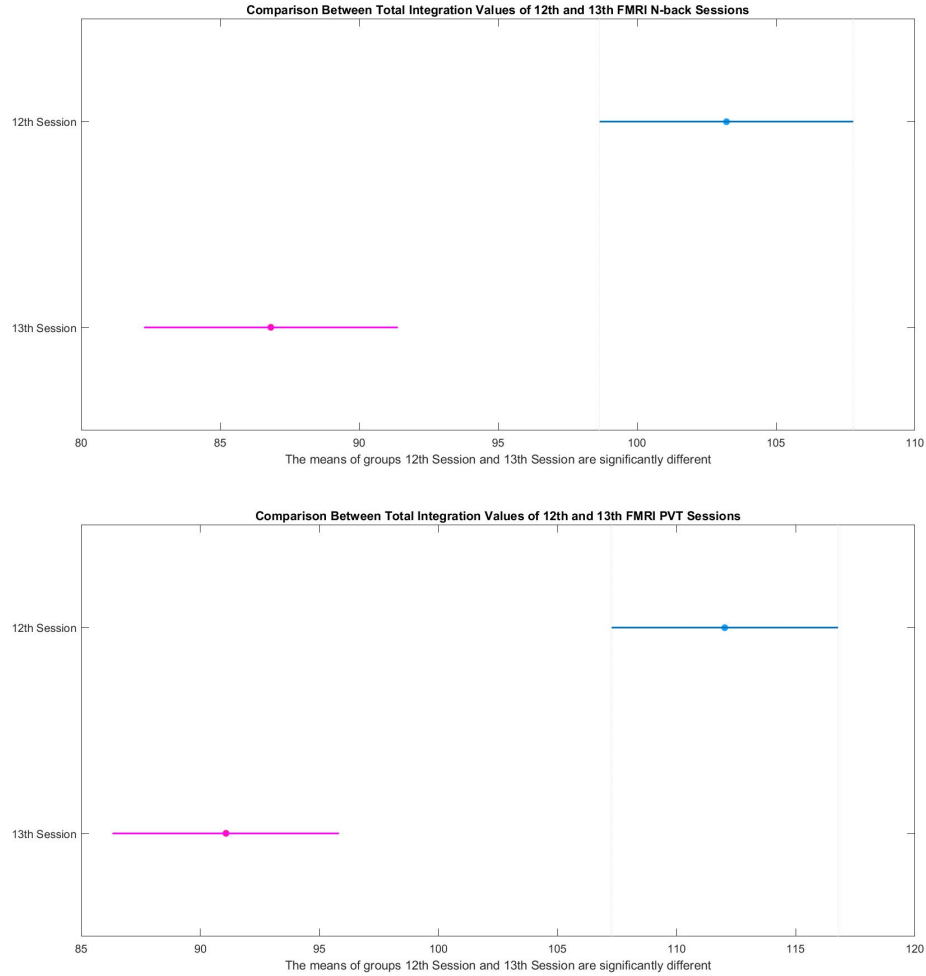
Figure 4.19: The ANOVA Results Between Total Integration of 12th and 13th FMRI Sessions - Pink Line is the 12th, and Blue Line is the 13th Session

In Figure 4.20, we compared the FCR values of the two last sessions in both N-back and PVT using the ANOVA test. Like the previous analysis, the pink line represents the FCR of all the subjects for the 12th session while the blue line is the FCR of all the subjects for the 13th session. This time in both N-back and PVT sessions, it is evident that the FCR's mean value for the 12th session (SD condition) is less than the 13th session (wakefulness condition). This suggests that the FCR increases after getting enough sleep.

In the last test case, we wanted to check if there are any differences between Morning Group
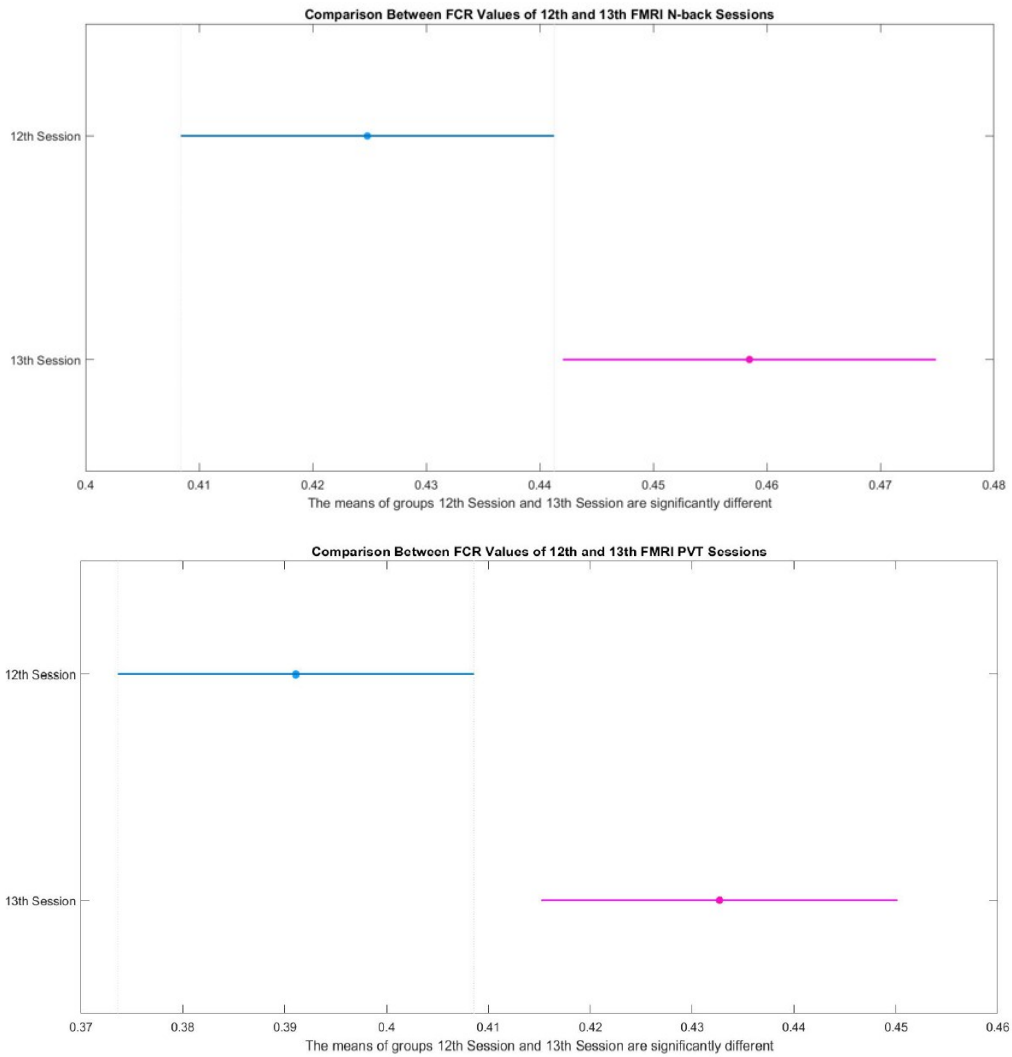
Figure 4.20: The ANOVA Results Between FCR of 12th and 13th FMRI Sessions - Pink Line is the 12th, and Blue Line is the 13th Session

and Evening Group when calculating the total integration. Figure 4.21 shows the results of this comparison. As shown in this figure, it seems that the total integration is higher in the Morning Group compared to the Evening Group.
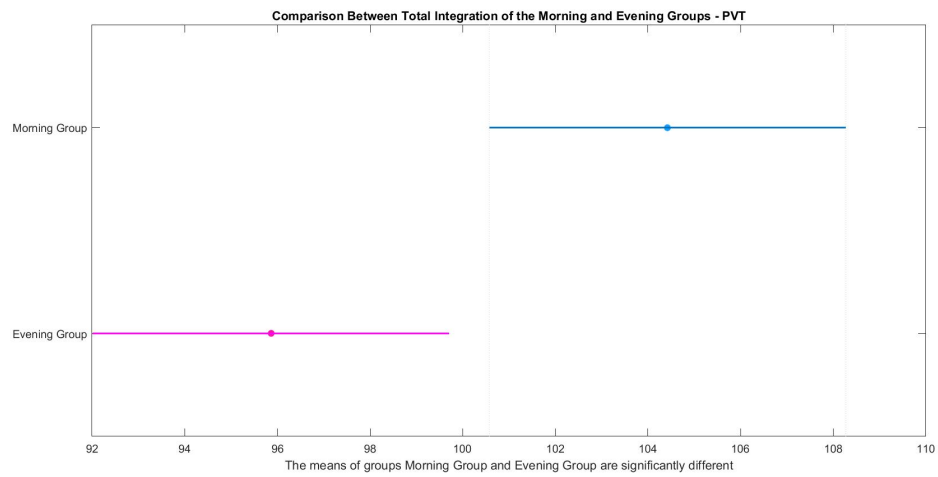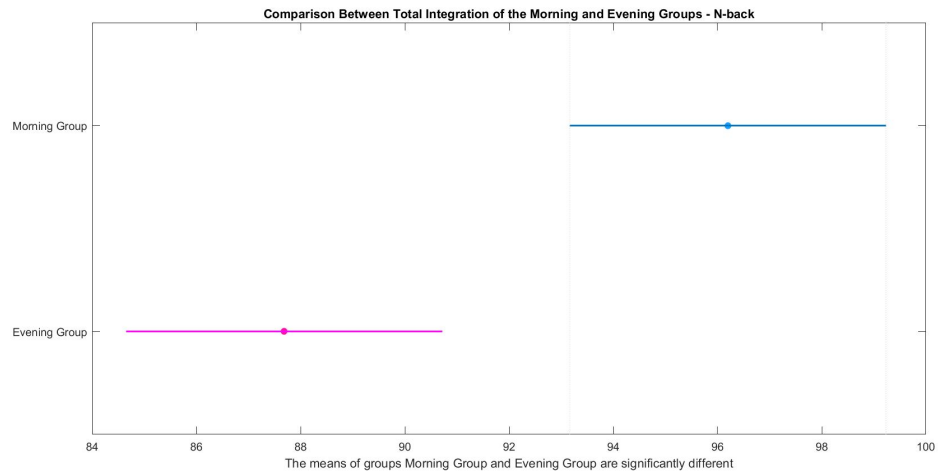
Figure 4.21: The ANOVA Results Between Total Integration of Morning and Evening Groups

Chapter 5

Conclusion and Future Work

5.1 Discussion

The goal of this thesis was to study the effects of sleep deprivation on the brain's functional integration and segregation. However, before computing those measures, we hypothesized that if the signals are not stationary, this may have some negative effects on our future calculations. As a result, we employed the sliding window approach with which we could go across the fMRI time-series to find the stationary parts of it. Afterward, we computed the rest of the analysis including the calculations of the hierarchical integration and FCR on the stationary parts of the signals. This method helped us in having fewer fluctuations in our results. The ADF test which we used for measuring the stationarity of the time-series is a very precise technique as it considers a possible drift and trend in the data. However, there are other parametric and non-parametric techniques that depending on a researcher's aim can be used for measuring the stationarity.

In this research, we calculated the hierarchical measure of integration which was introduced in [26], and then, calculated FCR which is introduced in [27]. As our primary goal was to study the whole brain's integration and segregation, we did not study any particular region of the brain. In [27], they computed FCR for wakefulness and NREM sleep. They observed that FCR increases during sleep which suggests that there is more modularity in the brain while asleep. In our sleep deprivation study, FCR decreased during the SD period. Afterward, we computed the FCR of the two last sessions (12 and 13), and observed that it increased after having 12 hours of recovery sleep.

This result supports the work of [27]. Contrary to FCR, the total integration increased during the SD period, and it decreased after the 12-hour recovery sleep.

The third goal we wanted to achieve in this research was to figure out if there is a linear relationship between the melatonin profile, and functional integration and FCR. Although in the GLM results, we could not find any proof of the existence of a linear connection, looking at the integration and melatonin curves at the subject level, we could see that the peaks of these two parameters were happening around the same period of time. However, for the other parts of the curves, some inconsistencies were observed in different subjects. The total integration curve was aligned with the melatonin curve for some of the subjects, but in others, they were not completely aligned. This can be due to some individual physiological differences or there might be another factor which has an effect on the integration curve that was not considered in this research.

In the last ANOVA test, We also observed a difference in the total integration results of Morning and Evening groups. Regardless of this result, both of these groups showed the same behavior in the results of functional integration and segregation. This difference in the level of their total integration can be due to not having equal sample size between these two groups.

5.2   Conclusion

In this thesis, we proved that performing stationarity analysis in studies that include statistical analysis is very crucial. It is inappropriate to assume that our fMRI time-series is completely stationary as there are some parts during which the mean or variance of the time-series is changing with time. Performing analysis on a non-stationary time-series leads to having noise and fluctuations in the results which is not desirable. For producing more reliable results, the best way is to find the parts in which the data is stationary and perform the analysis on those parts.

Furthermore, we showed the negative effects of sleep deprivation on a person's brain. In general, functional integration increases in SD and decreases again after getting enough sleep. On the contrary, FCR decreases in SD and increases after sleep. These findings suggest that SD disturbs the balance between functional integration and segregation. Moreover, as brain's modularity decreased

in SD condition, local neuronal groups in the brain were not acting in the same way as wakefulness condition. However, as the functional integration increased in SD, it shows that although the brain's modularity decreased, the flow of information between the brain's networks was more than the wakefulness condition. We can conclude that sleep plays a crucial role in balancing these two principles (functional integration and segregation).

5.3 Future Work

In this thesis, we performed our analysis on the entire data and did not choose any particular brain region. We can extend this work by selecting some regions of the brain and perform some analysis on the chosen networks.

(1) The stationarity analysis can be computed on chosen brain regions to see if we can see a significant difference in the results of different regions. If we see a huge difference, what does this non-stationarity mean for each region?

(2) The measure of integration and FCR can be computed for different brain regions to see if in a certain brain region, these parameters would show high circadian rhythmicity. Moreover, we can pinpoint in which brain regions we see more functional integration and segregation.

(3) Another interesting research for extending this work is to do the same analysis which was done in this study in a partial SD work. In a partial SD study, although the circadian rhythm is having its regular cycle which is not affected by prior sleep, sleep pressure would decrease by having a short nap during the day. In such a study, we could detect if the measure of integration is mostly showing circadian rhythmicity by following the melatonin curve, or after having a short nap, the measure of integration decreases as well.

(4) Lastly, as in some of the subjects there were some inconsistencies in the measure of integration, a study should be performed to detect the neurotransmitters such as glutamate, GABA, etc. which might have an effect in altering this parameter.

Bibliography

[1] G. Tononi, G. M. Edelman, and O. Sporns, "Complexity and coherency: integrating information in the brain," *Trends Cogn Sci.*, vol. 2, no. 12, pp. 474–484, Dec. 1998. [Online]. Available: https://pubmed.ncbi.nlm.nih.gov/21227298/

[2] G. Tononi, O. Sporns, and G. M. Edelman, "A measure for brain complexity: relating functional segregation and integration in the nervous system." *Proceedings of the National Academy of Sciences*, vol. 91, no. 11, pp. 5033–5037, May 1994. [Online]. Available: https://www.pnas.org/doi/abs/10.1073/pnas.91.11.5033

[3] J. M. Shine, "Neuromodulatory influences on integration and segregation in the brain," *Trends Cogn Sci.*, vol. 23, no. 7, pp. 572–583, Jul. 2019.

[4] G. Tononi and C. Cirelli, "Sleep and the price of plasticity: From synaptic and cellular homeostasis to memory consolidation and integration," *Elsevier Inc.*, vol. 18, no. 1, pp. 12–34, Jan. 2014. [Online]. Available: https://www.cell.com/neuron/fulltext/S0896-6273(13)01186-0?_returnURL=

[5] ——, "Sleep function and synaptic homeostasis," *Sleep Medicine Reviews*, vol. 10, no. 1, pp. 49–62, Feb. 2006. [Online]. Available: https://www.sciencedirect.com/science/article/pii/S1087079205000420

[6] NINDS, "Brain basics: Understanding sleep," https://www.ninds.nih.gov/health-information/patient-caregiver-education/brain-basics-understanding-sleep, Jul. 2022.

[7] M. Zhiqiang, C. Fan, J. Han, D. Wang, S. Di, W. Hu, D. Liu, X. Li, R. Reiter, and X. Yan, "Melatonin as a potential anticarcinogen for non-small-cell lung cancer," *Oncotarget*, vol. 7, Apr. 2016.

[8] R. Energy, "Melatonin for sleep," https://recharge.energy/en/melatonin-for-sleep/.

[9] L. Bullock, "Sleep-wake homeostasis: How our internal body clock regulates our sleep," https://www.mattressadvisor.com/how-homeostasis/, Jun. 2022.

[10] A. A. Borbély and P. Achermann, "Concepts and models of sleep regulation: an overview," *J. Sleep Res.*, vol. 1, no. 2, pp. 63–79, Jun. 1992. [Online]. Available: https://pubmed.ncbi.nlm.nih.gov/10607028/

[11] A. A. Borbély, S. Daan, A. Wirz-Justice, and T. Deboer, "The two-process model of sleep regulation: a reappraisal," *J. Sleep Res.*, vol. 25, no. 2, pp. 131–143, Apr. 2016. [Online]. Available: https://pubmed.ncbi.nlm.nih.gov/26762182/

[12] P. Alhola and P. Polo-Kantola, "Sleep deprivation: Impact on cognitive performance," *Neuropsychiatr Dis Treat.*, vol. 3, no. 5, p. 553–567, Oct. 2007. [Online]. Available: https://www.ncbi.nlm.nih.gov/pmc/articles/PMC2656292/

[13] W. D. S. Killgore, "Effects of sleep deprivation on cognition," *Prog Brain Res.*, vol. 185, pp. 105–129, 2010.

[14] A. Jegou, M. Schabus, O. Gosseries, B. Dahmen, G. Albouy, M. Desseilles, V. Sterpenich, C. Phillips, P. Maquet, C. Grova, and T. T. Dang-Vu, "Cortical reactivations during sleep spindles following declarative learning," *NeuroImage*, vol. 195, pp. 104–112, 2019. [Online]. Available: https://www.sciencedirect.com/science/article/pii/S1053811919302514

[15] N. Cross, C. Paquola, F. B. Pomares, A. A. Perrault, A. Jegou, A. Nguyen, U. Aydin, B. C. Bernhardt, C. Grova, and T. T. Dang-Vu, "Cortical gradients of functional connectivity are robust to state-dependent changes following sleep deprivation," *NeuroImage*, vol. 226, p. 117547, 2021. [Online]. Available: https://www.sciencedirect.com/science/article/pii/S1053811920310326

[16] F. V. Farahani, M. Fafrowicz, W. Karwowski, P. K. Douglas, A. Domagalik, E. Beldzik, H. Oginska, and T. Marek, "Effects of chronic sleep restriction on the brain functional network, as revealed by graph theory," *Sec. Neural Technology*, vol. 13, Oct. 2019.

[17] E. B. Simon, N. Lahav, R. Shamir, T. Hendler, and A. Maron-Katz, "Tired and misconnected: A breakdown of brain modularity following sleep deprivation," *Hum Brain Mapp.*, vol. 38, no. 6, pp. 3300–3314, Jun. 2017.

[18] B. T. Yeo, J. Tandi, and M. W. Chee, "Functional connectivity during rested wakefulness predicts vulnerability to sleep deprivation," *NeuroImage*, vol. 111, pp. 147–158, 2015. [Online]. Available: https://www.sciencedirect.com/science/article/pii/S1053811915001196

[19] Y. Lei, Y. Shao, L. Wang, E. Ye, X. Jin, F. Zou, T. Zhai, W. Li, and Z. Yang, "Altered superficial amygdala-cortical functional link in resting state after 36 hours of total sleep deprivation," *Neurosci Res.*, vol. 93, no. 12, pp. 1795–1803, Dec. 2015.

[20] O. G. Bosch, J. S. Rihm, M. Scheidegger, H.-P. Landolt, P. Stämpfli, J. Brakowski, F. Esposito, B. Rasch, and E. Seifritz, "Sleep deprivation increases dorsal nexus connectivity to the dorsolateral prefrontal cortex in humans," *Proceedings of the National Academy of Sciences*, vol. 110, no. 48, pp. 19 597–19 602, 2013. [Online]. Available: https://www.pnas.org/doi/abs/10.1073/pnas.1317010110

[21] S. A. Huettel, A. W. Song, and G. McCarthy, *Functional Magnetic Resonance Imaging*. Sinauer Associates is an imprint of Oxford University Press, 2014.

[22] G. H. Glover, "Overview of functional magnetic resonance imaging," *Neurosurg Clin N Am.*, vol. 22, no. 2, pp. 133–139, Apr. 2011.

[23] R. A. Poldrack, J. A. Mumford, and T. E. Nichols, *Handbook of Functional MRI Data Analysis*. Cambridge University Press, 2011.

[24] F. Liégeois and R. Elward, "Chapter 19 - functional magnetic resonance imaging," in *Neurocognitive Development: Disorders and Disabilities*, ser. Handbook of Clinical Neurology, A. Gallagher, C. Bulteau, D. Cohen, and J. L. Michaud, Eds. Elsevier, 2020,

vol. 174, pp. 265–275. [Online]. Available: https://www.sciencedirect.com/science/article/pii/B9780444641489000193

[25] K. Smitha, K. Raja, A. Karumattu Manattu, R. PG, B. Thomas, T. Kapilamoorthy, and C. Kesavadas, "Resting state fmri: A review on methods in resting state connectivity analysis and resting state networks," *Neuroradiol J.*, vol. 30, no. 4, pp. 305–317, Aug. 2017.

[26] G. Marrelec, P. Bellec, A. Krainik, H. Duffau, M. Pélégrini-Issac, S. Lehéricy, H. Benali, and J. Doyon, "Regions, systems, and the brain: Hierarchical measures of functional integration in fmri," *Medical Image Analysis*, vol. 12, no. 4, pp. 484–496, 2008. [Online]. Available: https://www.sciencedirect.com/science/article/pii/S1361841508000224

[27] M. Boly, V. Perlbarg, G. Marrelec, M. Schabus, S. Laureys, J. Doyon, M. Pélégrini-Issac, P. Maquet, and H. Benali, "Hierarchical clustering of brain activity during human nonrapid eye movement sleep," *Proceedings of the National Academy of Sciences*, vol. 109, no. 15, pp. 5856–5861, 2012. [Online]. Available: https://www.pnas.org/doi/abs/10.1073/pnas.1111133109

[28] V. Muto, M. Jaspar, C. Meyer, C. Kussé, S. L. Chellappa, C. Degueldre, E. Balteau, A. S.-L. Bourdiec, A. Luxen, B. Middleton, S. N. Archer, C. Phillips, F. Collette, G. Vandewalle, D.-J. Dijk, and P. Maquet, "Local modulation of human brain responses by circadian rhythmicity and sleep debt," *Science*, vol. 353, no. 6300, pp. 687–690, 2016. [Online]. Available: https://www.science.org/doi/abs/10.1126/science.aad2993

[29] G. E. P. Box, G. Jenkins, G. Reinsel, and G. Ljung, *Time Series Analysis, Forecasting and Control*.   John Wiley Sons, Inc., Hoboken, 1990.

[30] R. H. Shumway and D. S. Stoffer, *Time Series Analysis and Its Applications*.   Berlin, Heidelberg: Springer-Verlag, 2005.

[31] R. Sneiderman, "A quick introduction to time series analysis," https://towardsdatascience.com/a-quick-introduction-to-time-series-analysis-d86e4ff5fdd, Nov. 2020.

[32] M. Priestley, *Non-Linear and Non-Stationary Time Series Analysis*.   Academic Press, 1988.

[33] E. C. of Science, "Autoregressive models," https://online.stat.psu.edu/stat501/lesson/14/14.1.

[34] A. Bauer, "Automated hybrid time series forecasting: Design, benchmarking, and use cases," Ph.D. dissertation, 01 2021.

[35] S. Palachy, "Stationarity in time series analysis," https://towardsdatascience.com/stationarity-in-time-series-analysis-90c94f27322, Apr. 2019.

[36] W. Enders, *Applied Econometric Time Series*. John Wiley Sons, Inc., Hoboken, 2004.

[37] J. Breitung, "Nonparametric tests for unit roots and cointegration," *Journal of Econometrics*, vol. 108, no. 2, pp. 343–363, 2002. [Online]. Available: https://www.sciencedirect.com/science/article/pii/S0304407601001397

[38] S. Glen, "Unit root: Simple definition, unit root tests," https://www.statisticshowto.com/unit-root/.

[39] K. Patterson, *Unit Root Tests in Time Series*. Palgrave Macmillan, 2011.

[40] S. Glen, "Adf — augmented dickey fuller test," https://www.statisticshowto.com/adf-augmented-dickey-fuller-test/.

[41] Mathworks, "Sliding window method and exponential weighting method," https://www.mathworks.com/help/dsp/ug/sliding-window-method-and-exponential-weighting-method.html.

[42] GeeksforGeeks, "Window sliding technique," https://www.geeksforgeeks.org/window-sliding-technique/.

[43] A. Gelman and J. Hill, *Data Analysis Using Regression and Multilevel/Hierarchical Models*. New York: Cambridge University Press, 2006, vol. Analytical methods for social research.

[44] Mathworks, "Generalized linear models," https://www.mathworks.com/help/stats/generalized-linear-regression.html.

[45] A. Rutherford, *ANOVA and ANCOVA : a GLM approach*. Staffordshire, United Kingdom: Wiley, Hoboken, N.J., 2011.

[46] Mathworks, "One-way anova," https://www.mathworks.com/help/stats/one-way-anova.html.

[47] ——, "Two-way anova," https://www.mathworks.com/help/stats/two-way-anova.html.

[48] V. Muto, M. Jaspar, C. Meyer, C. Kussé, S. L. Chellappa, C. Degueldre, E. Balteau, A. S.-L. Bourdiec, A. Luxen, B. Middleton, S. N. Archer, C. Phillips, F. Collette, G. Vandewalle, D.-J. Dijk, and P. Maquet, "Supplementary materials for local modulation of human brain responses by circadian rhythmicity and sleep debt," *Science*, vol. 353, no. 6300, pp. 687–690, 2016. [Online]. Available: https://www.science.org/doi/abs/10.1126/science.aad2993

[49] D. J. Buysse, C. F. Reynolds, T. H. Monk, S. R. Berman, and D. J. Kupfer, "The pittsburgh sleep quality index: A new instrument for psychiatric practice and research," *Psychiatry Research*, vol. 28, no. 2, pp. 193–213, 1989. [Online]. Available: https://www.sciencedirect.com/science/article/pii/0165178189900474

[50] "Epworth sleepiness scale," https://epworthsleepinessscale.com/.

[51] Mayoclinic, "Polysomnography (sleep study)," https://www.mayoclinic.org/tests-procedures/polysomnography/about/pac-20394877.

[52] N. Goel, M. Basner, and D. F. Dinges, "Chapter thirteen - phenotyping of neurobehavioral vulnerability to circadian phase during sleep loss," in *Circadian Rhythms and Biological Clocks, Part B*, ser. Methods in Enzymology, A. Sehgal, Ed. Academic Press, 2015, vol. 552, pp. 285–308. [Online]. Available: https://www.sciencedirect.com/science/article/pii/S0076687914000251

[53] W. Kirchner, "Age differences in short-term retention of rapidly changing information," *Journal of Experimental Psychology*, vol. 55, no. 4, p. 352–358, 1958.

[54] A. Meule, "Reporting and interpreting working memory performance in n-back tasks," *Front Psychol.*, Mar. 2017.

[55] S. Urchs, J. Armoza, C. Moreau, Y. Benhajali, J. St-Aubin, P. Orban, and P. Bellec, "Mist: A multi-resolution parcellation of functional brain networks," *MNI Open Res.*, p. 1:3, 2019.

[56] Mathworks, "Adftest," https://www.mathworks.com/help/econ/adftest.html.